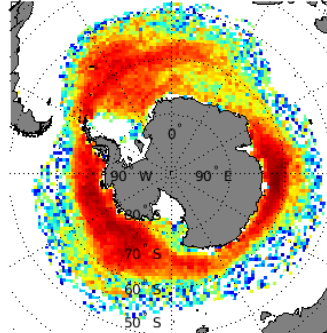




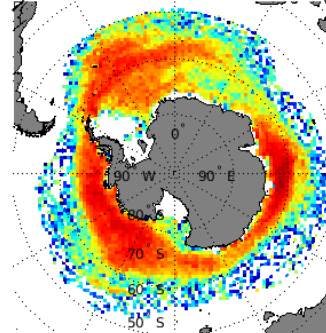
The ALTIBERG iceberg data base version 3.1, Antarctic and Arctic data sets

J. Tournadre, J.F. Piollé, M. Accensi, F. Girard-Ardhuin

Volume of ice 2010-2021 50km res



Volume of ice 2010-2021 100km res



Ref. : Doc.Tech.LOPS 2022-01

Version:3.1

Date: April 2022

Contents

1	The Antarctic and Arctic Altiberg small icebergs data base.	4
1.1	The altimeter missions	4
1.2	Detection method	5
1.2.1	Low resolution Mode	5
1.2.2	Iceberg area	7
1.2.3	Volume of ice	7
1.3	Merging the different altimeters	8
1.4	High resolution (HR) products	9
1.5	Distribution of iceberg length	9
1.6	Delay-Doppler or SAR data detection	10
1.6.1	SARIn mode size and freeboard estimates	10
1.7	Intercalibration the σ_0 and volume/	12
1.8	High resolution products	16
2	The data base products	20
2.1	Antarctic data set	23
2.1.1	Matlab files	23
2.1.1.1	Individual iceberg files	23
2.1.1.2	Gridded products	24
2.1.2	Netcdf files	25
2.1.2.1	Individual iceberg files	25
2.1.2.2	Merged iceberg files	28
2.1.2.3	Gridded products on regular latitude/longitude grid,	31
2.1.2.4	Gridded products on regular polar grid,	32
2.1.2.5	High resolution gridded products	34
2.2	Arctic data set	38
2.2.1	Matlab files	38
2.2.1.1	Individual iceberg files	38
2.2.1.2	Gridded products	39
2.2.2	Netcdf files	40
2.2.2.1	Individual iceberg files	40
2.2.2.2	Merged iceberg files	43

Altimeter version 3.1

Compared to the 3.0 version the 3.1 one includes 2021 and covers the 1992-2021 period. It should be noted that in September 2020 the HY-2A altimeter failed. However, in 2021 six altimeters are still in operations. The Sentinel6 satellite that was launched at the end of 2020 is not been yet included in the database. The Sentinel6 detection algorithm is under development and the data will be included in the near future.

Chapter 1

The Antarctic and Arctic Altimeter small icebergs data base.

1.1 The altimeter missions

A new altimeter have been added to the data base since version 2.3. The Haiyang 2B of the Chinese State Oceanic Administration satellite was launched in October 2018. It carries a dual frequency (Ku 13.58GHz and C 5.25GHz band) altimeter similar to the one on board its predecessor HY2A. The two satellites have a repeat period of 14days. Table 1.1 summarizes the main characteristics of the 15 altimeters used in ALTIBERG version 2.1.

Figure 1.1 shows the time-line of the different missions used. Since 1992 at least two altimeters are always available at any given time and since April 2010 at least 4. Since 2019, 7 altimeters are operational, even in this 3.1 version only 6 are processed in 2021.

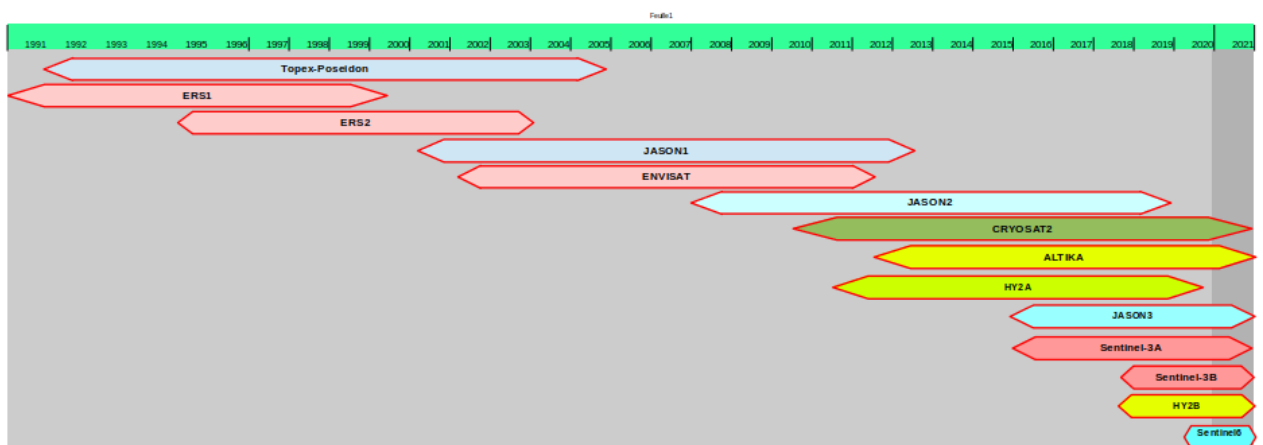


Figure 1.1: Time-line of the altimeter missions used in ALTIBERG

Altimeter	Time period	Altitude (km)	Inclination	Beam width	Frequency (GHz)	Numbers of bins	track point	bin width (ns)
ERS1	1992-1996	784	98°	1.3°	Ku- 13.8	64	32.5	3.03
ERS2	1995-2003	784	98°	1.3°	Ku-13.8	64	32.5	3.03
Topex	1992-2005	1334	66°	1.1°	Ku-13.6	128	32.5	3.125
Poseidon	1992-2005	1334	66°	1.1°	Ku-13.65	60	32.5	3.125
Jason1	2002-2012	1334	66°	1.3°	Ku-13.6	104	32.5	3.125
Envisat	2002-2012	784	98°	1.3°	Ku-13.575	128	43	3.125
Jason2	2008-	1334	66°	1.3°	Ku-13.5	104	32.5	3.125
Cryosat	2010-	717	92°	1.2°	Ku-13.575	128	34.5	3.125
Cryosat SAR	2010-	717	92°	1.2°	Ku-13.575	254	50	3.125
Cryosat-SARin	2010-	717	92°	1.2°	Ku-13.575	1024	252	3.125
ALTIKA	2013-	796	98.55°	0.61°	Ka-35.75	128	52	2.0
HY2A	2011-	963	99.3°	0.91°	Ku-13.58	128	32.5	3.125
Jason3	2016	1334	66	1.28°	Ku-13.5	104	32.5	3.125
Sentinel 3A	2016-	814.5	98.65°	1.2°	Ku-13.575	128	51	3.125
Sentinel 3B	2018-	814.5	98.65°	1.2°	Ku-13.575	128	51	3.125
HY2B	2018-	963	99.3°	1.02°	Ku 13.58	128	32.5	3.125
Geosat	1985-1989	757-814	108.1°	2°	Ku-13.5	63	32	3.125

Table 1.1: Main characteristics of the radar altimeters used to build the data base. In blue, new altimeters. In green the altimeters not included in the data base at present.

1.2 Detection method

Two iceberg detection algorithms are used in the database, one for the classical Low Resolution Mode of operation of altimeter and one for the Delay Doppler (SAR) mode of operation. The LRM and SAR detection methods used have been described in detail by Tournadre et al. [2008, 2012, 2018a]. They are only summarized in the present report.

1.2.1 Low resolution Mode

The LRM detection method is the one presented by Tournadre et al. [2008]. An altimeter is a nadir looking radar that emits short pulses that are backscattered by the sea surface. The altimeter measures the backscattered power as a function of time to construct the echo waveform from which the geophysical parameters are estimated. The backscatter coefficient of the waveform can be expressed as a double convolution product of the radar point target response, the flat sea surface response and the joint probability density function of slope and elevation of the sea surface Brown [1977]. The radar cross section for backscatter as a function of time, $\sigma(t)$, assuming a Gaussian altimeter pulse, a Gaussian antenna pattern and a Gaussian random distribution of rough-surface specular points, can be expressed as Barrick and Lipa [1985]

$$\sigma(t) = \frac{1}{2}(2\pi)^{3/2} H'' \sigma_\tau \sigma_0 \left(1 + \operatorname{erf} \left(\frac{x}{\sqrt{2}\sigma_p} \right) \right) e^{-\frac{x}{u_b}} \quad (1.1)$$

where $x = ct/2$, $H'' = H/(1 + H/a)$ is the reduced satellite height, a being the earth's radius, and H the satellite height. σ_τ is the standard deviation of the altimeter pulse; $\sigma_p = \sqrt{h^2 + \sigma_\tau^2}$ where h is the rms wave height; u_b is the antenna pattern standard deviation; σ_0 is the target backscatter coefficient. It should be noted that $t = 0$ corresponds to the mean sea level. The measured Jason-1 waveforms are given in telemetry samples of 3.125 ns width (the length of the pulse) and the nominal track point (i.e. the sea level or $t=0$) is shifted to bin 32.5.

A point target of height δ above sea level located at distance d from the satellite nadir will give an echo at the time t_0 defined by (Powell et al. [1993])

$$\frac{ct_0}{2} = -\delta + \frac{1}{2} \frac{a + H}{aH} d^2 = -\delta + \frac{d^2}{2H''} \quad (1.2)$$

The echo waveform of a point target is purely deterministic, i.e. a parabola as a function of time. Using the radar equation (Roca et al. [2003]) it is of the form

$$\sigma_{target}(t) = \frac{\sigma_1}{2\pi^2 H^4 (1 + \frac{d^2}{2H^2})} e^{-\frac{u_0}{u_b}} e^{-\frac{(x+\delta-u_0)^2}{2\sigma_\tau^2}}, \quad (1.3)$$

where σ_1 is the target radar cross section, and $u_0 = \frac{d^2}{2H''}$.

For an iceberg of area A and constant surface backscatter coefficient σ_1 , the waveform is obtained by summation of (1.3) over A

$$\sigma_{ice}(t) = \frac{\sigma_1}{2\pi^2 H^4} \oint_A \frac{1}{1 + \frac{d^2}{2H^2}} e^{-\frac{u_0}{u_b}} e^{-\frac{(x+\delta-u_0)^2}{2\sigma_\tau^2}} dA \quad (1.4)$$

To be detectable in echo waveforms, an iceberg should have an echo at a time, t_0 that lies within the time range during which the echo waveform is integrated, i.e. for Jason-1 between the telemetry sample 1 and 30. The target backscatter coefficient should also be large enough to come out of the thermal noise of the sensor.

The signature of icebergs is always characterized by the parabolic shape defined by (1.2). The automated detection is based on the analysis of the convolution product C between a filter, F characteristic of an iceberg signature, and the thermal noise sections of the waveforms.

$$C(i, j) = \sum_{n=1}^{30} \sum_{m=1}^{M_2} \sigma_0(i, j) F(i - n, j - m) \quad (1.5)$$

where i is the telemetry sample index, j , the waveform index, and $\sigma_0(i, j)$, the j^{th} waveform. The filter used has been computed by the waveform model of (1.4) for a 100x100 m² iceberg.

For each waveform, the maximum of correlation $C(j)$ and its location $i_{max}^C(j)$ (i.e. the range), and the maximum of backscatter, $\sigma_{max}(j)$ and its location $i_{max}^\sigma(j)$ are determined. A waveform is assumed to contain an iceberg signature if $C_{max}(j)$ and $\sigma_{max}(j)$ are larger than given thresholds C_1 and σ_1 .

For each signature a maximum of 40 waveforms can be involved Tournadre et al. [2008]. If n consecutive waveforms are detected as containing a signature, the time of the echo (t_{ech}) is estimated as

$$t_{ech} = (32.5 - \min(i_{max}^\sigma(j), j = 1..n)) * 3.125 \quad (1.6)$$

and the iceberg backscatter, σ_{iceb} , is estimated as the maximum observed backscatter of the whole signature, i.e.

$$\sigma_{iceb} = \max(\sigma_{max}(j), j = 1..n) \quad (1.7)$$

1.2.2 Iceberg area

The method of detection provides the time of the echo (i.e. the range) as well as the mean backscatter. The range depends on the distance d from nadir of the iceberg center and on the free-board elevation h of the iceberg. The mean backscatter depends not only on the area, A , and on the distance from nadir but also on the backscattering coefficient of the iceberg surface, σ_0^{ice} , which is conditioned by the ice characteristics, the shape and roughness of the iceberg surface, and the presence on the iceberg surface of snow or water. The two parameters, t_{ech} and σ_{iceb} , are thus function of four main unknowns, d , A , h and σ_0^{ice} . The iceberg area can be estimated if assumptions are made on the values of two of the remaining unknowns (d , h σ_0^{ice}).

The backscatter coefficient of the iceberg surface is assumed to be the same for all icebergs. Using studies published on the analysis of Envisat Ku-band backscatter over ice caps Legresy et al. [2005], Tran et al. [2008, 2009] the iceberg surface backscatter σ_1 has been set at 19 dB Tournadre et al. [2012].

Secondly, it is necessary to fix either a mean distance from nadir of the icebergs or a mean iceberg free-board elevation. As the distance from nadir is a purely random variable with uniform probability, we choose to assume a constant free-board elevation. Following Gladstone et al. [2001], Romanov et al. [2012] the free-board elevation for icebergs larger than 200 m, is set at 28 m corresponding to a mean iceberg thickness of 250 m.

Using the fixed free-board and surface backscatter assumptions, an analytical model of waveforms has been used to compute the signature of square icebergs as a function of distance from nadir, (0 to 12 km), and area (0.01 to 9 km²). The time of the echo $t_{ech} = f(d, A)$ and the mean backscatter $\sigma_{iceb} = g(d, A)$ have been estimated from the modeled waveforms and were then used to compute an inverse model $A = l(t_{ech}, \sigma_{iceb})$ and $d = m(t_{ech}, \sigma_{iceb})$.

The inverse model is applied to the range and backscatter of the detected icebergs to estimate the area and distance from nadir.

1.2.3 Volume of ice

The iceberg data set is then used to compute the monthly probability of presence $P(i, j, t)$ (t being the month), over a regular polar stereographic grid (i, j) as well as the mean monthly iceberg area, $A(i, j, t)$

$P(i, j, t)$ is simply the ratio of the number N of icebergs detected within a grid cell by the number N_s of valid Jason-1 samples within the same grid cell

$$P(i, j) = N(i, j)/N_s(i, j) \quad (1.8)$$

and $A(i, j, t)$ is defined as

$$A(i, j, t) = \frac{1}{N(i, j, t)} \sum_{k=1}^{N(i, j, t)} a_k$$

Tournadre et al. [2008] where a_k are the areas of the $N(i, j, t)$ icebergs detected within the grid cell (i, j) during month t .

The total area of the iceberg detected within a grid cell (i, j) is simply

$$S(i, j, t) = \sum_{k=1}^{N(i, j, t)} a_k$$

and as the iceberg thickness H_T is assumed constant, the detected volume of ice is $S(i, j, t)H_T$.

The detected volume of ice per unit area of the grid cell is the ratio of the detected volume of ice to the total area sampled by the altimeter over month t , i.e. $S(i, j, t)H_T / (A_{SW}N_s(i, j, t))$ where A_{SW} is the area of an altimeter footprint and $N_s(i, j, t)$ is the number of valid altimeter samples. Assuming that the monthly iceberg distribution within a grid cell is uniform, the total volume of ice within the grid cell is the product of the volume per unit area by the area of the grid cell, i.e

$$V(i, j, t) = \frac{S(i, j, t)H_T}{A_{SW}N_s(i, j, t)} \Delta x \Delta y \quad (1.9)$$

The area of the altimeter footprint for the detection of 28 m free-board icebergs A_{SW} is the product of the altimeter along track resolution (290 m) by the range of distance from nadir over which an iceberg can be detected. Using the relationship between the time of the echo, the distance from nadir and the elevation of a target emerging from the sea given by Tournadre et al. [2008], the range of detection of an iceberg is given by

$$\sqrt{(ct_0 + 2h)H''} + \frac{\bar{d}_0}{2} \geq d \geq \sqrt{(ct_1 + 2h)H''} - \frac{\bar{d}_0}{2} \quad (1.10)$$

where $H'' = H / (1 + H/a)$ is the reduced satellite altitude, a being the earth's radius and H the satellite altitude, h is the iceberg free-board elevation, c is the speed of light, d_0 is the mean iceberg length, and t_0 and t_1 are the time limits of the noise range part of the waveform. For Jason-1, $H = 1340$ km and $t_0 = -32 \times 3.125$ ns and $t_1 = -2 \times 3.125$ ns, then 8.24 km $> d > 4.85$ km, thus $A_{SW} \simeq 5.8 \times 3.5 \times 2$ km², where factor 2 accounts for the left-right ambiguity of detection.

1.3 Merging the different altimeters

The products from the different sensors are also merged to produce an homogeneous time series of probability, mean area and volume of ice. The merged products is obtained by a weighted sum of the individual products, i.e. for the volume of ice

$$V_m(i, j, t) = \sum_{i=1}^n V_i(i, j, t) * w_i \quad (1.11)$$

where the weights w_i are given by

$$w_i = \frac{N(i, j, t)_i}{\sum_{i=1}^n N_i(i, j, t)} \quad (1.12)$$

where N_i is the number of valid data for the satellite i and n is the number of satellites available at time t .

1.4 High resolution (HR) products

Since 2010, at least 4 altimeters are always operating at the same time and among these 4 altimeters at least 2 have a high inclination orbit (thus covering latitudes over 66°). This allows a very good coverage of the polar regions and make it possible to increase the time and space resolution of the merged gridded products. Starting in 2010, three new high resolution products are available for the Southern Ocean

- 50 km regular polar grid, 14 days (thus 26 date per year)
- 100 km regular polar grid, 14 days
- 1x1° latitude longitude grid, 14 days.

For the Greenland data-set, the resolution is already 50 km for the regular polar grid. Because of the small number of icebergs, it is necessary to have at least 6 altimeters operating at the same time to allow to decrease the time resolution to 14 day. A new products at 50 km and 14 days resolutions starting in 2016 will be released in version 4.

The HR products are computed using the method described for the monthly products presented in 1.2.3. For each satellite, the probability of presence, the mean area, the volume of ice and the number of valid samples are computed at the given time and space resolution. The fields of the different satellite are then merged using the method of 1.3.

The individual satellite HR fields are significantly noisier than the monthly one are thus not distributed. **Only the merged with or without the Cryosat SARin products are distributed.**

1.5 Distribution of iceberg length

As suggested by Wadhams [1988] for iceberg length, the area distribution follows in general quite well a two-parameter log-normal distribution f_X of the form

$$f_X(x; \mu, \sigma) = \frac{1}{x\sigma\sqrt{2\pi}} e^{-\frac{(\ln x - \mu)^2}{2\sigma^2}} \&, \quad x > 0 \quad (1.13)$$

where μ and σ are the location and scale parameters respectively. For each grid cell, the yearly distribution of iceberg length is estimated and a The Maximum Likelihood Estimations (MLE) is used to compute μ and σ^2 . The mean of the distribution is then defined by $e^{\mu + \frac{\sigma^2}{2}}$.

1.6 Delay-Doppler or SAR data detection

The Delay-Doppler (or SAR) mode detection algorithm, also used for SAR Interferometric (SARIn) mode, has been described in details by Tournadre et al. [2018a]. It is summarized in this paragraph to better explain the software changes for Cryosat-SAR and SARIn mode data.

Compared to LRM data, the incoherent summation use to produce the stacked SAR mode echoes strongly reduces the noise level of the waveforms Thermal Noise Part (above the surface) used for detection. It can be considered as negligible, which facilitates the detection. To enhance the iceberg signatures, the waveforms are normalized by the mean waveform (\overline{WF}) and rms (σ_{WF}) computed for each altimeter cycle,

$$WF'(i, j) = (WF(i, j) - \overline{WF}(j)) / \sigma_{WF}(j) \quad (1.14)$$

A binary image is then created by thresholding WF' at 4 (i.e. $4\sigma_{WF}$). The image Connected Components (CC's) are computed using a classical graph theory algorithm such as the Matlab© *bwconncomp* or SCiPy *label* routines. The CC's properties; area, position, mean and max backscatter; are then estimated using Matlab© or SCiPy *regionprops* routines. The algorithm allows to detect the bright spots associated to the iceberg signatures in the SAR waveforms. The icebergs area can be estimated using the maximum backscatter in the same way as it is done for LRM data and using the same backscatter model.

The icebergs area can also be estimated from the size of SAR signature. While the along-track resolution is 300 m, the across-track resolution depends on free-board elevation and distance from nadir). For example, icebergs with a 28 m free-board can only be detected if their distance from nadir ranges from 2 to 7 km [Tournadre et al., 2016]. Between 2 and 7 km, the SAR range bin width, dy , varies from ~ 200 to ~ 20 m. Two area estimates are computed, the first one is the sum of the CC's area multiplied by the along track and across-track resolution

$$a_i = \sum_j s_j dx dy \quad (1.15)$$

where s_i are the area (in pixels) of the CCs associated to the iceberg, and dx and dy are along and across-track resolutions. The second method assumes that the iceberg's length in range, l_y , extends from the minimum to the maximum range values of the CC's detected at the same along-track location while the width, w_x , is the along-track width. The iceberg's area is thus

$$A_i = w_x dx l_y dy \quad (1.16)$$

The range bin width, dy is then used to compute minimum and maximum values of the two area estimates. The calibration of SAR volume estimates is thus conducted by adjusting the dy value. The second method is used in the ALTIBERG data base.

1.6.1 SARIn mode size and freeboard estimates

The principles of interferometric altimetry were first proposed by Jensen [1999]. A detailed description of the principles and processing of the Cryosat SARIn data is given in Wingham et al. [2006]. The main (left) antenna transmits the radar signal and the two antennas measure the

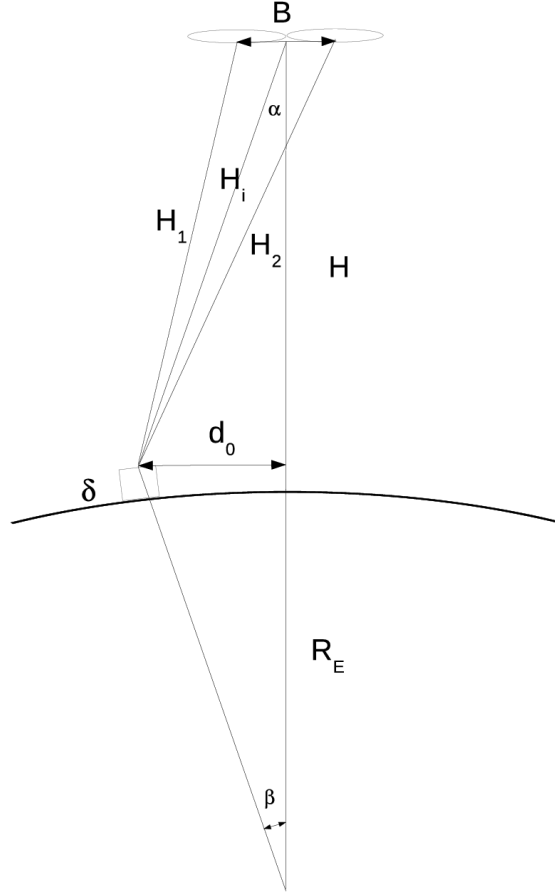


Figure 1.2: Cryosat-2 SARIn geometry. B : Baseline, i.e. distance between the two antennas, d_0 distance of the iceberg from nadir, δ iceberg's free-board, R_E earth's radius, H satellite altitude, H_1, H_2 ranges of iceberg for the two antennas. α off-nadir angle.

backscattered echo waveform (see Figure 1.2). The main complex waveform is multiplied with the complex conjugate of the second antenna waveform. The phase of the resulting cross-channel waveform is then defined as the interferometric phase difference, which results from the slight range difference of an off-nadir scatterer for the two antennas. The normalized modulus of the conjugate product gives the estimate of the signal coherence. The stacked SAR echoes for both antennas are computed using the SAR mode processing. In SARIn mode the waveform analysis window is increased to 512 bins (240 m) to better sample sloping terrains. In the Baseline-C data products used in this study, the use of zero-padding prior to FFT processing further increase the number of range bins to 1024 without changing the range window. Each bin corresponds thus to 1.565 ns or 0.23 m in range. The thermal noise part of the waveforms used for iceberg detection is 230 bins long.

The interferometric phase difference, $\Delta\psi$, is related to the off-nadir angle, α , by

$$\Delta\Psi = \frac{2\pi B}{\lambda} \sin(\alpha) \quad (1.17)$$

where λ is the radar wavelength and B is interferometer baseline (distance between the two

antennas). Under the small angle approximation, the off-nadir angle α is

$$\alpha = \frac{\lambda \Delta \Psi}{2\pi B} \quad (1.18)$$

Galim et al. [2013] estimated an angle scaling factor a ($\alpha' = \alpha/a$) to compensate slight differences between the two SIRAL antennas. The across-track distance to nadir, d_0 , is given

$$d_0 = H_i \alpha' \quad (1.19)$$

where H_i is the range defined by $H_i = ct_i/2$, t_i being the pulse two-way travel time.

Taking the earth's curvature into account, an iceberg detected in range bin b_1 , corresponding to travel time t_1 , and at off-nadir α_1 , has a free-board given by [Nanda, 2015]

$$\delta = (H - H_i \cos \alpha_1 + R_E (1 - \cos \beta)) \cos \beta \quad (1.20)$$

where $\beta = H/R_E \alpha_1$ and $H_i = ct_1/2$.

The SARin echoes are similar to the SAR ones, except that the number of range bins in the echoes TNP is significantly larger (115x2 vs 50). The swath over which icebergs can be detected which is of the order of 6 km is thus significantly increased to ~ 10 km. The SAR detection algorithm can be applied to the SARin waveforms without modification. However, in the echoes TNP the signals received by the two antennas are by nature random noise and thus incoherent.

The estimated phase difference is thus a random noise while the coherence should be 0. If a target emerges from the sea surface, the signals received by the antennas becomes coherent. High coherence values indicate the presence of scatterers and are used to further improve the detection and decrease the probability of false alarm. Only samples with coherence larger than 0.7 are considered to construct the binary image used for detection.

The SARin detected signatures are irregularly spaced across-track and need to be re-sampled on a regular grid in order to geographically map the iceberg location, free-board and backscatter. The chosen grid is regular in the along- and across-track directions with an along-track resolution of 300 m (i.e. the distance between two consecutive waveforms) and an across-track resolution of 50 m. The latitude and across-track distance of detected iceberg pixel are remapped on the regular grid using classical earth's projections. The icebergs characteristics are then estimated by analyzing the Connected Components and regions properties of the remapped free-board and backscatter fields.

1.7 Intercalibration the σ_0 and volume/

Forth both the Arctic and Antarctic icebergs the 17 data sets corresponding to the 15 altimeters have been inter-calibrated using the procedure described in Tournadre et al. [2016] and in the previous ALTIBERG documents Tournadre et al. [2013, 2015, 2018b]. Figure 1.3 compare the calibrated σ_0 , distance from nadir and area of the different altimeters.

Tables 1.2 and 1.3 compares the version 2 and 3 detection parameters and calibration coefficients for the antarctic and arctic icebergs. The new intercalibration only slightly modifies the 20Hz calibration coefficients.

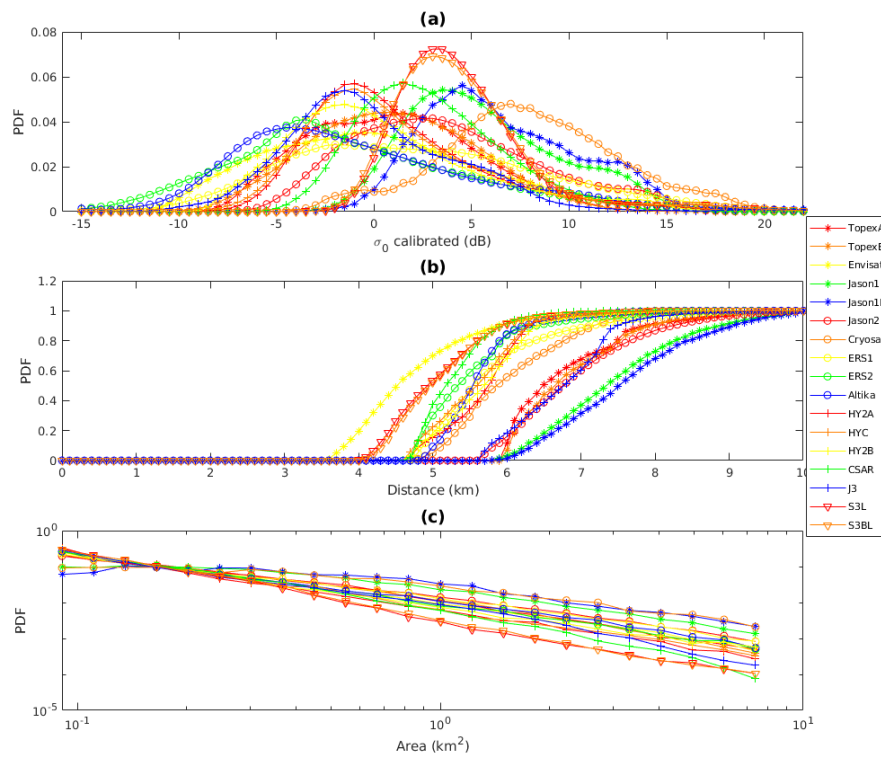


Figure 1.3: (Top) PDF of calibrated σ_0 , (middle) of distance from nadir and (bottom) area.

1.7. Intercalibration the σ_0 and volume of the Antarctic and Arctic Altiberg small icebergs data base.

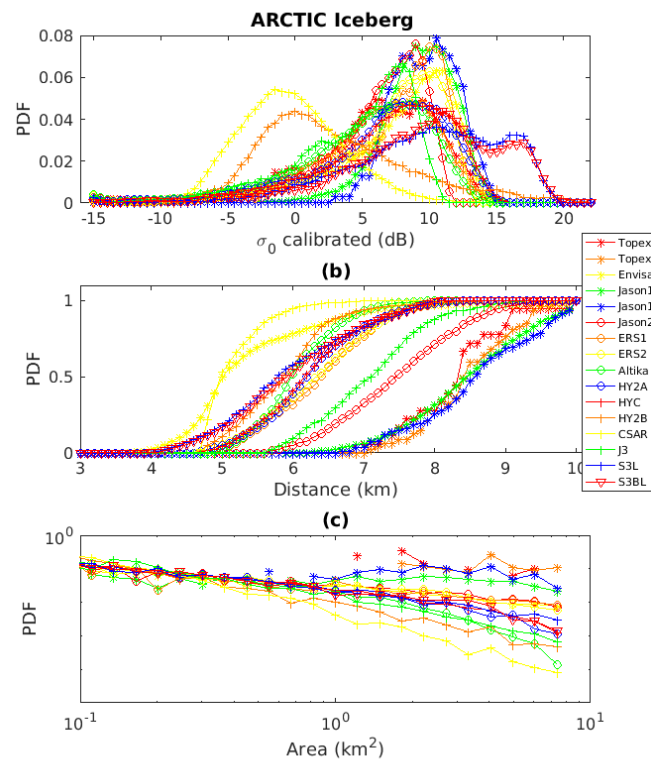


Figure 1.4: (Top) PDF of calibrated σ_0 , (middle) of distance from nadir and (bottom) area.

Altimeter	Usable bins	1hz σ_0 Cal. vs Jason1 (dB)	20Hz σ_0 Cal. version2.1	20Hz σ_0 Cal. version3	A_{SW} km^2
ERS1	6-27	2.7	0.4	0.4	19.8
ERS2	7-27	2.7	0.2	0.2	19.8
Topex	7-27	2.4	0(A)-0(B)	0(A)-0(B)	28.5
Poseidon	-	-	-	-	-
Jason1	5-24	0	-1	-1	34.8
Envisat	7-39	2.9	1.5	1	41.2
Jason2	3-24	0	-0.5	0.3	37.7
Cryosat	13-45	2.9	0	4	20
Cryosat SAR	3-40	2.9	$dy = 100m$	$dy = 100m$	20
Cryosat SARIN	30-230	2.9	-	-	TBD
ALTIKA	13-48	0	-0.8	-0.8	26.2
Haiyang-2A	1-24	0	2.5-2.5(CNES)	2.5 -2.5(CNES)	23.7
Jason-3	3-24	0	-0.5	0.5	37.7
Sentinel-3 (A&B)PLRM	2-40	2.9	-	3.5	27.6
Sentinel-3 (A&B)SAR	2-40	2.9	-	$dy = 160m$	27.6
Haiyang-2B	26-28	0	-	0	23.7
Geosat	2-26	+3.1	0		16.5

Table 1.2: Antarctic detection parameters for the different versions. Cal.; calibration, A_{SW} , surface normalization coefficient.

<i>Altimeter</i>	<i>Usable bins</i>	<i>1hz σ_0 Cal. vs Jason1 (dB)</i>	<i>20Hzσ_0 Cal. version2.3 (dB)</i>	<i>20Hzσ_0 Cal. version3 (dB)</i>	<i>A_{SW} km²</i>
<i>ERS1</i>	<i>14-26</i>	<i>2.7</i>	<i>-1.0</i>	<i>-0.5</i>	<i>23.8</i>
<i>ERS2</i>	<i>14-26</i>	<i>2.7</i>	<i>-0.5</i>	<i>-0.5</i>	<i>23.8</i>
<i>Topex</i>	<i>8-26</i>	<i>2.4</i>	<i>1(A)-1(B)</i>	<i>1(A)-1(B)</i>	<i>34.1</i>
<i>Poseidon</i>	<i>-</i>	<i>-</i>	<i>-</i>	<i>-</i>	<i>-</i>
<i>Jason1</i>	<i>5-24</i>	<i>0</i>	<i>-1.0</i>	<i>-0</i>	<i>34.8</i>
<i>Envisat</i>	<i>7-39</i>	<i>2.9</i>	<i>0.5</i>	<i>0.5</i>	<i>38.0</i>
<i>Jason2</i>	<i>3-24</i>	<i>0</i>	<i>0</i>	<i>1</i>	<i>36.6</i>
<i>Cryosat</i>	<i>13-45</i>	<i>2.9</i>	<i>0</i>	<i>0</i>	<i>19.2</i>
<i>Cryosat SAR</i>	<i>3-30</i>	<i>2.9</i>	<i>dy = 100m</i>	<i>dy = 100m</i>	<i>19.2</i>
<i>Cryosat SARIN</i>	<i>30-230</i>	<i>2.9</i>	<i>-</i>	<i>-</i>	<i>38.4</i>
<i>ALTIKA</i>	<i>13-48</i>	<i>0</i>	<i>-0.8</i>	<i>-0.8</i>	<i>28.4</i>
<i>HY-2A</i>	<i>1-24</i>	<i>1</i>	<i>0-0(CNES)</i>	<i>1.5-1.5(CNES)</i>	<i>23.7</i>
<i>Jason-3</i>	<i>3-24</i>	<i>0</i>	<i>0.5</i>	<i>0</i>	<i>37.7</i>
<i>Sentinel-3A SAR</i>	<i>2-40</i>	<i>2.9</i>	<i>dy = 160m</i>	<i>dy = 160m</i>	<i>27.6</i>
<i>Sentinel-3A PLRM</i>	<i>2-40</i>	<i>2.9</i>	<i>3.5</i>	<i>3.5</i>	<i>27.6</i>
<i>Sentinel-3B SAR</i>	<i>2-40</i>	<i>2.9</i>	<i>dy = 160m</i>	<i>dy = 160m</i>	<i>27.6</i>
<i>Sentinel-3B PLRM</i>	<i>2-40</i>	<i>2.9</i>	<i>3.5</i>	<i>3.5</i>	<i>27.6</i>
<i>HY-2B</i>	<i>1-28</i>	<i>0</i>	<i>0</i>	<i>0</i>	<i>23.7</i>
<i>Geosat</i>	<i>2-26</i>	<i>3.1</i>	<i>0</i>	<i>0</i>	<i>16.5</i>

Table 1.3: Version 3 Detection parameters for the Arctic data set, usable bins in the thermal noise part of the waveforms, 1hz and 20 Hz calibration, A_{SW} , surface normalization coefficient.

Figures 1.5 and 1.6 present the calibrated and uncalibrated time variations of σ_0 , mean area and slope of the area distributions for all sensors. These plots shows that there is no significant drift of backscatter, mean area and slope of the size distribution during the period considered for each sensor.

Figures 1.7 and 1.8 compare the inter-calibrated total volume of ice of the 16 altimeters data sets for the southern Ocean and the Greenland sea respectively.

1.8 High resolution products

Starting in 2010, the new high resolution fortnightly products allows a more detailed description of the geographical distribution of the small icebergs around Antarctica as it can be seen in figure 1.10 that presents the 2010-2020 total volume of ice at 100 and 50 km resolution.

It is for example possible to better identify the emissary glaciers, the impact of the circulation around the Balleny Islands, as well as the impact of the Weddell Sea gyre on the distribution of the iceberg.

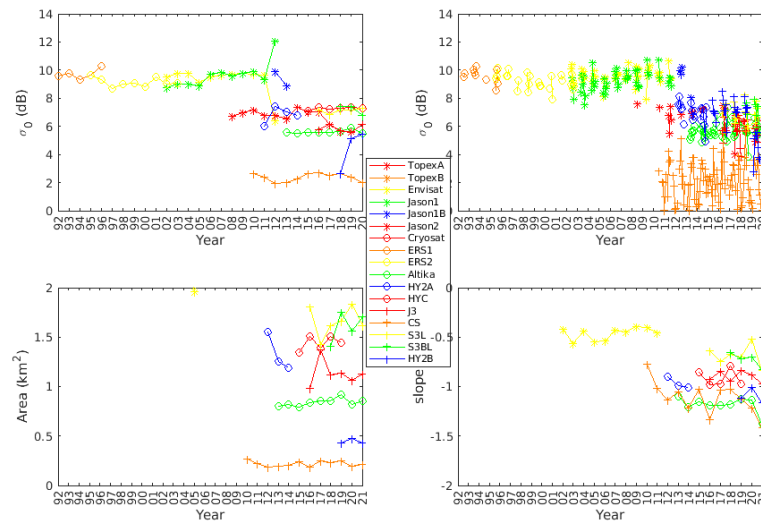


Figure 1.5: Time variation of yearly (top, left) and monthly (top right) calibrated σ_0 . Time variation of the mean annual area (bottom left) and σ_0 and slope of the size distribution (bottom right) for the Arctic data set

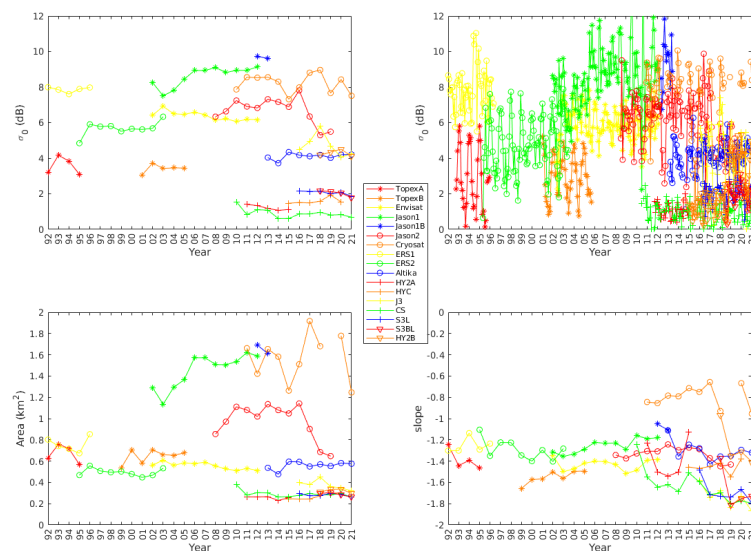


Figure 1.6: Time variation of yearly (top, left) and monthly (top right) calibrated σ_0 . Time variation of the mean annual area (bottom left) and σ_0 and slope of the size distribution (bottom right) for the Antarctic data set.

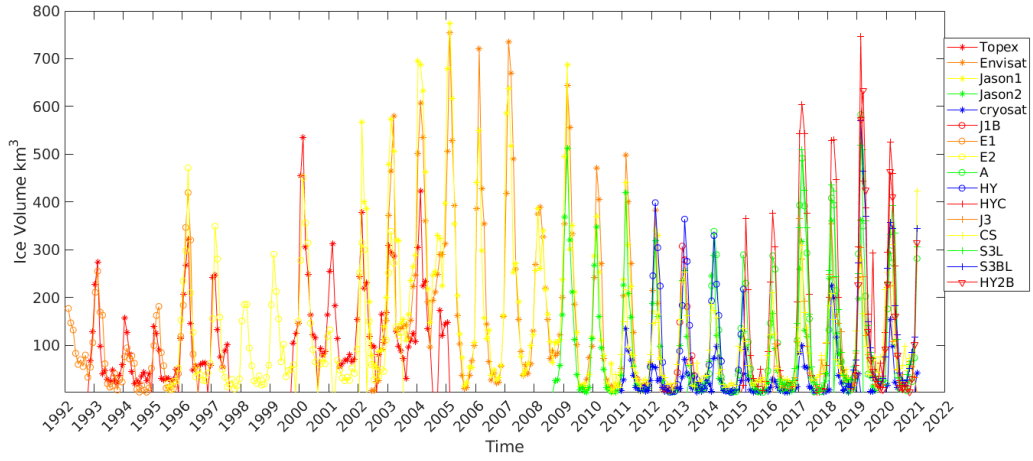


Figure 1.7: Comparison of the total ice volume for all the altimeters for the southern ocean.

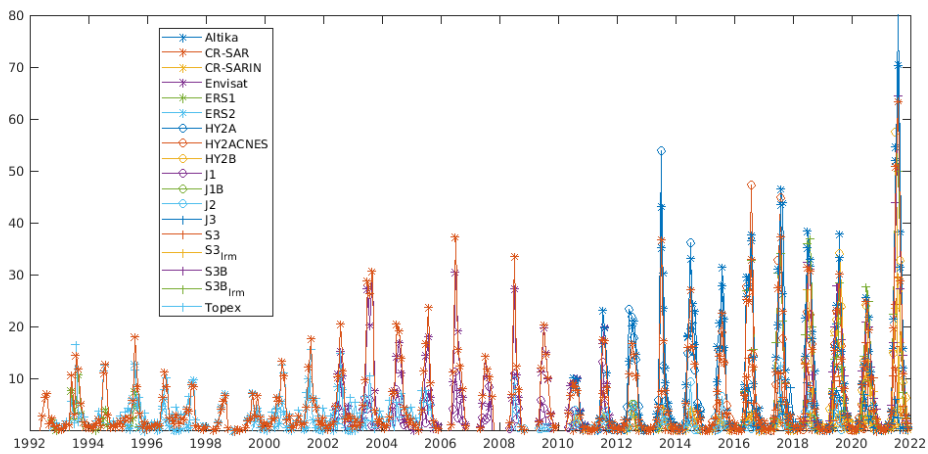


Figure 1.8: Comparison of the total ice volume for all the altimeters for the Greenland seas.

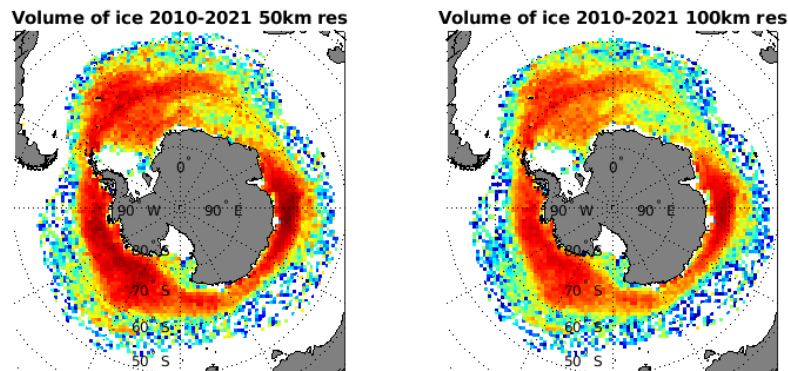


Figure 1.9: Total volume of ice in the Southern Ocean from the HR 50 km, 100km and 1x1° biweekly mean field and from the LR 100 km monthly one.

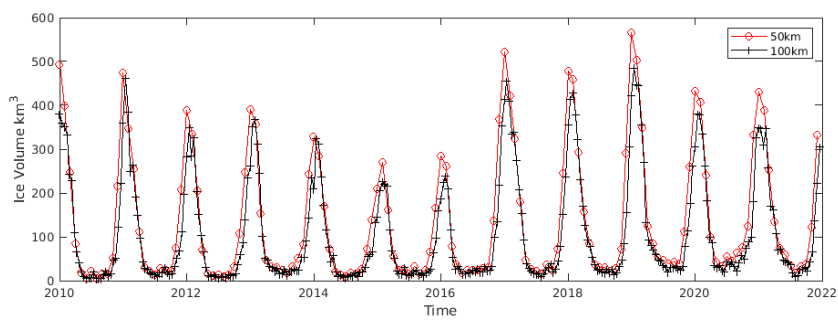


Figure 1.10: Total volume of ice from 2010 to 2020 at 100 km (left) end 50 km (right).

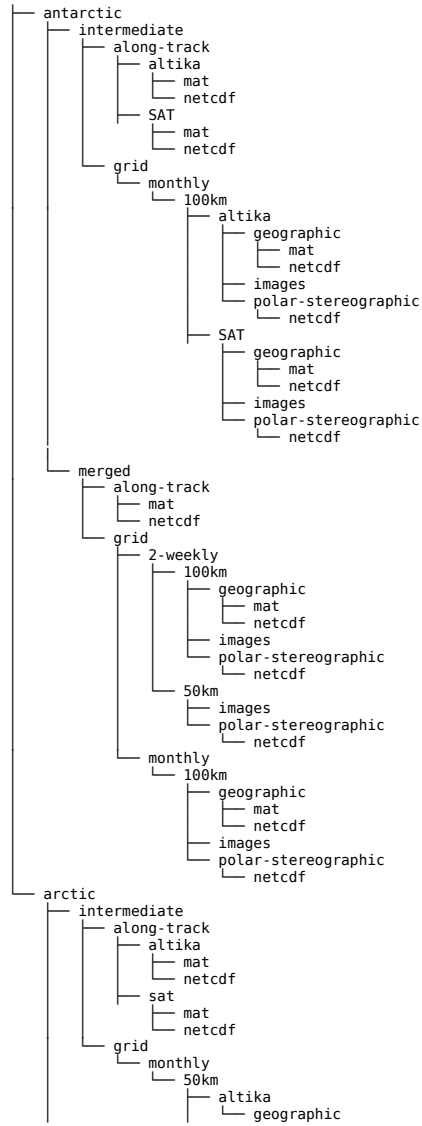
The total biweekly volume of ice at the different HR resolution and at the LR 100 km monthly resolution is presented in figure 1.9. The good agreement between the different time and space resolutions shows the robustness of the estimation of the volume of ice.

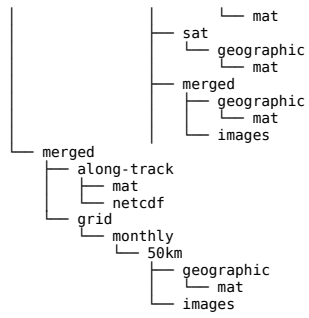
Chapter 2

The data base products

The data base is organized first by regions: **Antarctic** and **Arctic**, and by **satellite mission**. The files for the two regions are different, mainly because the number of icebergs is much smaller for the Arctic.

- SAT name of satellite





IMPORTANT NOTICE

For a general use, the HR merged gridded products are located at

<ftp://ftp.ifremer.fr/ifremer/cersat/projects/altiberg/v3/data/antarctic/merged/grid/2-weekly>
and the regular monthly products are located at

<ftp://ftp.ifremer.fr/ifremer/cersat/projects/altiberg/v3/data/antarctic/merged/grid/monthly>

The arctic data set is located at

<ftp://ftp.ifremer.fr/ifremer/cersat/projects/altiberg/v3/data/arctic/merged/montly>

The antarctic and arctic merged individual icebergs data set (along-track) are located at

<ftp://ftp.ifremer.fr/ifremer/cersat/projects/altiberg/v3/data/antarctic/merged/along-track/>

<ftp://ftp.ifremer.fr/ifremer/cersat/projects/altiberg/v3/data/arctic/merged/along-track/>

The full merged data set require to download only the two following directories

<ftp://ftp.ifremer.fr/ifremer/cersat/projects/altiberg/v3/data/antarctic/merged/>

and

<ftp://ftp.ifremer.fr/ifremer/cersat/projects/altiberg/v3/data/arctic/merged/>

2.1 Antarctic data set

2.1.1 Matlab files

2.1.1.1 Individual iceberg files

filename convention: `iceberg_sat_year.mat`

- *sat* : (*ers1,ers2,topex, envisat, jason1, jason1b, jason2,cryosat, cryosatSAR, cryosatSARIn, sentinel3A, sentinel3ALRM, sentinel3B, sentinel3BLRM, HY2B,merged*)
- *year* : four digit year ex : 2001

Variables

- *ic_anne* year
- *ic_mois* month
- *ic_jour* day
- *ic_Tjul* time in julian day (matlab format)
- *ic_CYCL* satellite cycle number
- *ic_TR* satellite track number
- *ic_lat* latitude
- *ic_lon* longitude (0 360°)
- *ic_LambX* polar Lambert coordinates X
- *ic_LambY* : polar Lambert coordinates Y

- *ic_ Jecho* Position of the echo : range bin of the echo (from convolution)
- *ic_ Jk* Position of the echo : range bin of the echo (from waveforms)
- *ic_ conc* Sea ice concentration from monthly mean SSM/I fields (%)
- *ic_ sig* Iceberg backscatter (dB)
- *ic_ sig_ cal* Calibrated Iceberg backscatter (dB)
- *ic_ surf* Iceberg area (km²)
- *ic_ surf_ cal* Calibrated Iceberg area (km²)
- *ic_ di* Distance from nadir (km)
- *ic_ di_ cal* Calibrated Distance from nadir (km)
- *ic_ sat* satellite that detected the iceberg (**for merged files only**)
- *ic_ fre* iceberg max freeboard (m) (**CRYOSAT SARIN only**)
- *ic_ frem* iceberg mean freeboard (m) (**CRYOSAT SARIN only**)
- *ic_ sat* satellite that detected the iceberg (**for merged files only**), ers1, 2 ers2; 3 topex; 4 jason1; 5 jason2; 6 jason1b; 7 cryosat; 8 envisat; 9 Altika, 10 HY2A; 11 HY2ACNES, 12 jason3; 13 cryosatSAR; 14 Sentinel3ALRM; 15 Sentinel3BLRM; 16 Cryosat; 17 cryosat-sarin, 18 HY2B

2.1.1.2 Gridded products

filename convention prod_gridded_sat_year.mat

- *sat* : (**ers1,ers2,topex, envisat, jason1, jason1b, jason2,jason3,altika, cryosat, cryosatSAR, cryosatSARIn, sentinel3A, sentinel3ALRM, sentinel3B, sentinel3BLRM, HY2B, n**)
- *year* : four digit year ex : 2001

The polar grid is a regular grid of 100 km x100km cells from -7000 to +7000 km from the pole. The lat/lon grid is 1°latitude by 2° longitude from 90°S to 40°S and 0 to 360°E.

Variables

- LAT : Latitudes of the cells
- LON: Longitudes of the cell
- Nicelalo : Monthly (12) Probability of presence of iceberg on the regular lat/lon grid
- SURFICelalo : Monthly (12) Mean surface of iceberg on the regular lat/lon grid
- VOLLalo : Monthly (12) Volume of ice on the regular lat/lon grid
- alat : Latitude of the regular polar grid

- `alon` : Longitude of the regular polar grid
- `Nice` : Monthly (12) Probability of presence of iceberg on the regular polar grid
- `SURFICElalo` : Monthly (12) Mean surface of iceberg on the regular polar grid
- `VOLLalo` : Monthly (12) Volume of ice on the regular polar grid
- `mle` : Mean yearly length of the iceberg obtained from by fitting a log-normal distribution on the histogram of the lengths within the grid cell (*set to 0 for merged products*)
- `mle` : μ parameter of the log-normal distribution (*set to 0 for merged products*)
- `smle` : σ^2 of the log-normal distribution (*set to 0 for merged products*)
- `surf_norm` : surface of the altimeter swath (km²) (*set to 0 for merged products*)

2.1.2 Netcdf files

2.1.2.1 Individual iceberg files

netcdf filename convention: `iceberg_sat_year.nc`

- `sat` : (*ers1,ers2,topex, envisat, jason1, jason1b, jason2,jason3,altika,cryosat, cryosatSAR, sentinel3A, sentinel3ALRM, sentinel3B, sentinel3BLRM,HY2A,HY2A_CNES*)
- `year` : four digit year ex : 2001

```
netcdf iceberg_envisat_2011 {
dimensions:
    time = 7766 ;
variables:
    int time(time) ;
        time:units = "days since 1990-01-01T00:00:00Z" ;
        time:long_name = "julian day (UT)" ;
        time:standard_name = "time" ;
        time:conventions = "Relative julian days" ;
        time:axis = "T" ;
    float lat(time) ;
        lat:long_name = "latitude" ;
        lat:standard_name = "latitude" ;
        lat:units = "degree_north" ;
        lat:valid_min = -90. ;
        lat:valid_max = 90. ;
        lat:_FillValue = 9.96921e+36f ;
        lat:content = "T" ;
        lat:associates = "time" ;
    float lon(time) ;
        lon:long_name = "longitude" ;
        lon:standard_name = "longitude" ;
        lon:units = "degree_east" ;
        lon:valid_min = -180. ;
        lon:valid_max = 180. ;
```

```

lon: _FillValue = 9.96921e+36f ;
lon: content = "T" ;
lon: associates = "time" ;
float lambx(time) ;
lambx: long_name = "x coordinate in lambert south pole projection" ;
lambx: standard_name = "projection_x_coordinate" ;
lambx: units = "km" ;
lambx: valid_min = 0. ;
Le 09/04/2021 à 20:21, Jean-François Piollé a écrit : > oui on a prévu une mise à jour tou
> Le 09/04/2021 à 14:50, Jean TOURNADRE a écrit : >> Salut Michael >> Altiberg va être inc
>>> tu pourrais faire automatiser au cersat pour que ce soit actualisé tout les mois ? >>>
lambx: valid_max = 10000. ;
lambx: _FillValue = 9.96921e+36f ;
lambx: content = "T" ;
lambx: associates = "time" ;
float lamby(time) ;
lamby: long_name = "y coordinate in lambert south pole projection" ;
lamby: standard_name = "projection_y_coordinate" ;
lamby: units = "km" ;
lamby: valid_min = 0. ;
lamby: valid_max = 100. ;
lamby: _FillValue = 9.96921e+36f ;
lamby: content = "T" ;
lamby: associates = "time" ;
float cycle(time) ;
cycle: long_name = "satellite cycle number" ;
cycle: units = "n/a" ;
cycle: valid_min = 0. ;
cycle: valid_max = 1000. ;
cycle: _FillValue = 9.96921e+36f ;
cycle: content = "T" ;
cycle: associates = "time" ;
float pass_number(time) ;
pass_number: long_name = "satellite pass number" ;
pass_number: units = "n/a" ;
pass_number: valid_min = 0. ;
pass_number: valid_max = 100. ;
pass_number: _FillValue = 9.96921e+36f ;
pass_number: content = "T" ;
pass_number: associates = "time" ;
float j_conv(time) ;
j_conv: long_name = "range bin of the iceberg echo (convolution)" ;
j_conv: units = "n/a" ;
j_conv: valid_min = 0. ;
j_conv: valid_max = 100. ;
j_conv: _FillValue = 9.96921e+36f ;
j_conv: content = "T" ;
j_conv: associates = "time" ;
float j_wf(time) ;
j_wf: long_name = "range bin of the iceberg echo (waveform)" ;
j_wf: units = "n/a" ;
j_wf: valid_min = 0. ;
j_wf: valid_max = 100. ;
j_wf: _FillValue = 9.96921e+36f ;
j_wf: content = "T" ;

```

```

        j_wf:associates = "time" ;
float sigma0(time) ;
    sigma0:long_name = " iceberg backscatter at Ku band" ;
    sigma0:units = "dB" ;
    sigma0:valid_min = 0. ;
    sigma0:valid_max = 100. ;
    sigma0:_FillValue = 9.96921e+36f ;
    sigma0:content = "T" ;
    sigma0:associates = "time" ;
float surface(time) ;
    surface:long_name = "iceberg surface" ;
    surface:units = "km2" ;
    surface:valid_min = 0. ;
    surface:valid_max = 1000. ;
    surface:_FillValue = 9.96921e+36f ;
    surface:content = "T" ;
    surface:associates = "time" ;
float distance(time) ;
    distance:long_name = "distance of the iceberg from nadir" ;
    distance:units = "km" ;
    distance:valid_min = 0. ;
    distance:valid_max = 100. ;
    distance:_FillValue = 9.96921e+36f ;
    distance:content = "T" ;
    distance:associates = "time" ;
float sigma0_cal(time) ;
    sigma0_cal:long_name = "iceberg backscatter at Ku band calibrated" ;
    sigma0_cal:units = "dB" ;
    sigma0_cal:valid_min = 0. ;
    sigma0_cal:valid_max = 100. ;
    sigma0_cal:_FillValue = 9.96921e+36f ;
    sigma0_cal:content = "T" ;
    sigma0_cal:associates = "time" ;
float surface_cal(time) ;
    surface_cal:long_name = "iceberg surface from calibrated backscatter" ;
    surface_cal:units = "km2" ;
    surface_cal:valid_min = 0. ;
    surface_cal:valid_max = 100. ;
    surface_cal:_FillValue = 9.96921e+36f ;
    surface_cal:content = "T" ;
    surface_cal:associates = "time" ;
float distance_cal(time) ;
    distance_cal:long_name = "distance of the iceberg from nadir using the c
    distance_cal:units = "db" ;
    distance_cal:valid_min = 0. ;
    distance_cal:valid_max = 100. ;
    distance_cal:_FillValue = 9.96921e+36f ;
    distance_cal:content = "T" ;
    distance_cal:associates = "time" ;
float sea_ice_conc(time) ;
    sea_ice_conc:long_name = " Daily sea ice concentration from SSMI" ;
    sea_ice_conc:standard_name = "sea_ice_area_fraction" ;
    sea_ice_conc:units = "%" ;
    sea_ice_conc:valid_min = 0. ;
    sea_ice_conc:valid_max = 100. ;

```

```

    sea_ice_conc: _FillValue = 9.96921e+36f ;
    sea_ice_conc: content = "T" ;
    sea_ice_conc: associates = "time" ;

// global attributes :
    :source = "ENVISAT SGDR" ;
    :project = "Altiberg " ;
    :authors = "J. Tournadre & M. Accensi" ;
    :contact = "cersat@ifremer.fr" ;
    :start_date = "20110101T000000" ;
    :stop_date = "20111201T000000" ;
    :field_type = "yearly" ;
    :sensor = "envisat" ;
}

```

2.1.2.2 Merged iceberg files

netcdf filename convention: iceberg_sat_year.nc

- o *sat* : (**merged**)

- o *year* : four digit year ex : 2001

- o

```

netcdf iceberg_merged_2003 {
dimensions :
    time = 25719 ;
variables :
    int time(time) ;
        time:units = "days since 1990-01-01T00:00:00Z" ;
        time:long_name = "julian day (UT)" ;
        time:standard_name = "time" ;
        time:conventions = "Relative julian days" ;
        time:axis = "T" ;
    float lat(time) ;
        lat:long_name = "latitude" ;
        lat:standard_name = "latitude" ;
        lat:units = "degree_north" ;
        lat:valid_min = -90. ;
        lat:valid_max = 90. ;
        lat:_FillValue = 9.96921e+36f ;
        lat:content = "T" ;
        lat:associates = "time" ;
    float lon(time) ;
        lon:long_name = "longitude" ;
        lon:standard_name = "longitude" ;
        lon:units = "degree_east" ;
        lon:valid_min = -180. ;
        lon:valid_max = 180. ;
        lon:_FillValue = 9.96921e+36f ;
        lon:content = "T" ;
        lon:associates = "time" ;
    float lambx(time) ;
        lambx:long_name = "x coordinate in lambert south pole projection" ;

```

```

    lambx:standard_name = "projection_x_coordinate" ;
    lambx:units = "km" ;
    lambx:valid_min = 0. ;
    lambx:valid_max = 10000. ;
    lambx:_FillValue = 9.96921e+36f ;
    lambx:content = "T" ;
    lambx:associates = "time" ;
float lamby(time) ;
    lamby:long_name = "y coordinate in lambert south pole projection" ;
    lamby:standard_name = "projection_y_coordinate" ;
    lamby:units = "km" ;
    lamby:valid_min = 0. ;
    lamby:valid_max = 100. ;
    lamby:_FillValue = 9.96921e+36f ;
    lamby:content = "T" ;
    lamby:associates = "time" ;
float cycle(time) ;
    cycle:long_name = "satellite cycle number" ;
    cycle:units = "n/a" ;
    cycle:valid_min = 0. ;
    cycle:valid_max = 1000. ;
    cycle:_FillValue = 9.96921e+36f ;
    cycle:content = "T" ;
    cycle:associates = "time" ;
float pass_number(time) ;
    pass_number:long_name = "satellite pass number" ;
    pass_number:units = "n/a" ;
    pass_number:valid_min = 0. ;
    pass_number:valid_max = 100. ;
    pass_number:_FillValue = 9.96921e+36f ;
    pass_number:content = "T" ;
    pass_number:associates = "time" ;
float j_conv(time) ;
    j_conv:long_name = "range bin of the iceberg echo (convolution)" ;
    j_conv:units = "n/a" ;
    j_conv:valid_min = 0. ;
    j_conv:valid_max = 100. ;
    j_conv:_FillValue = 9.96921e+36f ;
    j_conv:content = "T" ;
    j_conv:associates = "time" ;
float j_wf(time) ;
    j_wf:long_name = "range bin of the iceberg echo (waveform)" ;
    j_wf:units = "n/a" ;
    j_wf:valid_min = 0. ;
    j_wf:valid_max = 100. ;
    j_wf:_FillValue = 9.96921e+36f ;
    j_wf:content = "T" ;
    j_wf:associates = "time" ;
float sigma0(time) ;
    sigma0:long_name = "iceberg backscatter at Ku band" ;
    sigma0:units = "dB" ;
    sigma0:valid_min = 0. ;
    sigma0:valid_max = 100. ;
    sigma0:_FillValue = 9.96921e+36f ;
    sigma0:content = "T" ;

```

```

        sigma0:associates = "time" ;
float surface(time) ;
    surface:long_name = "iceberg surface" ;
    surface:units = "km2" ;
    surface:valid_min = 0. ;
    surface:valid_max = 1000. ;
    surface:_FillValue = 9.96921e+36f ;
    surface:content = "T" ;
    surface:associates = "time" ;
float distance(time) ;
    distance:long_name = "distance of the iceberg from nadir" ;
    distance:units = "km" ;
    distance:valid_min = 0. ;
    distance:valid_max = 100. ;
    distance:_FillValue = 9.96921e+36f ;
    distance:content = "T" ;
    distance:associates = "time" ;
float sigma0_cal(time) ;
    sigma0_cal:long_name = "iceberg backscatter at Ku band calibrated" ;
    sigma0_cal:units = "dB" ;
    sigma0_cal:valid_min = 0. ;
    sigma0_cal:valid_max = 100. ;
    sigma0_cal:_FillValue = 9.96921e+36f ;
    sigma0_cal:content = "T" ;
    sigma0_cal:associates = "time" ;
float surface_cal(time) ;
    surface_cal:long_name = "iceberg surface from calibrated backscatter" ;
    surface_cal:units = "km2" ;
    surface_cal:valid_min = 0. ;
    surface_cal:valid_max = 100. ;
    surface_cal:_FillValue = 9.96921e+36f ;
    surface_cal:content = "T" ;
    surface_cal:associates = "time" ;
float distance_cal(time) ;
    distance_cal:long_name = "distance of the iceberg from nadir using the
    distance_cal:units = "db" ;
    distance_cal:valid_min = 0. ;
    distance_cal:valid_max = 100. ;
    distance_cal:_FillValue = 9.96921e+36f ;
    distance_cal:content = "T" ;
    distance_cal:associates = "time" ;
float sea_ice_conc(time) ;
    sea_ice_conc:long_name = " Daily sea ice concentration from SSM/I" ;
    sea_ice_conc:standard_name = "sea_ice_area_fraction" ;
    sea_ice_conc:units = "%" ;
    sea_ice_conc:valid_min = 0. ;
    sea_ice_conc:valid_max = 100. ;
    sea_ice_conc:_FillValue = 9.96921e+36f ;
    sea_ice_conc:content = "T" ;
    sea_ice_conc:associates = "time" ;
float sat(time) ;
    sat:long_name = "'satellite that detected the iceberg , 1 ers1 , 2 ers2
    9 Altika , 10 HY2A; 11 HY2ACNES, 12 jason3; 13 cryosatSAR; 1
    17 cryosatsarin; 18 HY2B')";
    sat:standard_name = "satellite" ;

```

```

    sat:units = "-" ;
    sat:scale_factor = 1. ;
    sat:valid_max = 8. ;
    sat:_FillValue = 9.96921e+36f ;
    sat:content = "T" ;
    sat:associates = "time" ;

// global attributes:
    :source = "MERGED SGDR" ;
    :project = "Altiberg " ;
    :authors = "J. Tournadre & M. Accensi" ;
    :contact = "cersat@ifremer.fr" ;
    :start_date = "20030101T000000" ;
    :stop_date = "20031201T000000" ;
    :field_type = "yearly" ;
    :sensor = "merged" ;
}

```

2.1.2.3 Gridded products on regular latitude/longitude grid,

Netcdf filename convention prod_latlon_sat_year.nc

- o *sat* : (*ers1,ers2,topex, envisat, jason1, jason1b, jason2,jason3,altika,cryosat, cryosatSAR, cryosatSARIn, sentinel3A, sentinel3ALRM, sentinel3B, sentinel3BLRM,HY2E*)
- o *year* : four digit year ex : 2001

```

netcdf prod_latlon_envisat_2011 {
dimensions:
    time = 12 ;
    longitude = 181 ;
    latitude = 51 ;
variables:
    int time(time) ;
        time:units = "days since 1990-01-01T00:00:00Z" ;
        time:long_name = "julian day (UT)" ;
        time:standard_name = "time" ;
        time:conventions = "Relative julian days" ;
        time:axis = "T" ;
    double longitude(longitude) ;
        longitude:long_name = "longitude" ;
        longitude:standard_name = "longitude" ;
        longitude:units = "degree_east" ;
        longitude:valid_min = "-180" ;
        longitude:valid_max = "180" ;
        longitude:axis = "X" ;
    double latitude(latitude) ;
        latitude:long_name = "latitude" ;
        latitude:standard_name = "latitude" ;
        latitude:units = "degree_north" ;
        latitude:valid_min = "-90" ;
        latitude:valid_max = "90" ;
}

```

```

        latitude:axis = "Y" ;
float probability(time, longitude, latitude) ;
    probability:long_name = "probability of presence of iceberg" ;
    probability:units = "1/km2" ;
    probability:valid_min = 0. ;
    probability:valid_max = 1. ;
    probability:_FillValue = 9.96921e+36f ;
    probability:content = "TYX" ;
    probability:associates = "time latitude longitude" ;
float ice_volume(time, longitude, latitude) ;
    ice_volume:long_name = "volume of ice" ;
    ice_volume:units = "GigaTons" ;
    ice_volume:valid_min = 0. ;
    ice_volume:valid_max = 100. ;
    ice_volume:_FillValue = 9.96921e+36f ;
    ice_volume:content = "TYX" ;
    ice_volume:associates = "time latitude longitude" ;
float ice_area(time, longitude, latitude) ;
    ice_area:long_name = "mean area of iceberg" ;
    ice_area:units = "km2" ;
    ice_area:valid_min = 0. ;
    ice_area:valid_max = 100. ;
    ice_area:_FillValue = 9.96921e+36f ;
    ice_area:content = "TYX" ;
    ice_area:associates = "time latitude longitude" ;
float ice_length(longitude, latitude) ;
    ice_length:long_name = "mean length of iceberg from a log normal fit of pd
    ice_length:units = "km" ;
    ice_length:valid_min = 0. ;
    ice_length:valid_max = 2000. ;
    ice_length:_FillValue = 9.96921e+36f ;
    ice_length:content = "YX" ;
    ice_length:associates = "latitude longitude" ;

// global attributes :
    :source = "ENVISAT SGDR" ;
    :project = "Altiberg" ;
    :authors = " J. Tournadre & M. Accensi " ;
    :contact = "cersat@ifremer.fr" ;
    :southernmost_latitude = -90. ;
    :northernmost_latitude = -40. ;
    :latitude_resolution = 1. ;
    :westernmost_longitude = 0. ;
    :easternmost_longitude = 360. ;
    :longitude_resolution = 2. ;
    :start_date = "20110101T000000" ;
    :stop_date = "20111201T000000" ;
    :field_type = "monthly" ;
    :sensor = "envisat" ;
}

```

2.1.2.4 Gridded products on regular polar grid,

netcdf filename convention prod_polar_sat_year nc{

sat : (*ers1,ers2,topex, envisat, jason1, jason1b, jason2,jason3,altika,cryosat, cryosat-SAR, cryosatSARln, sentinel3A, sentinel3ALRM, sentinel3B, sentinel3BLRM, merged*)
year : four digit year ex : 2001

```
netcdf prod_latlon_envisat_2011 {
dimensions:
    time = 12 ;
    longitude = 181 ;
    latitude = 51 ;
variables:
    int time(time) ;
        time:units = "days since 1990-01-01T00:00:00Z" ;
        time:long_name = "julian day (UT)" ;
        time:standard_name = "time" ;
        time:conventions = "Relative julian days" ;
        time:axis = "T" ;
    double longitude(longitude) ;
        longitude:long_name = "longitude" ;
        longitude:standard_name = "longitude" ;
        longitude:units = "degree_east" ;
        longitude:valid_min = "-180" ;
        longitude:valid_max = "180" ;
        longitude:axis = "X" ;
    double latitude(latitude) ;
        latitude:long_name = "latitude" ;
        latitude:standard_name = "latitude" ;
        latitude:units = "degree_north" ;
        latitude:valid_min = "-90" ;
        latitude:valid_max = "90" ;
        latitude:axis = "Y" ;
    float probability(time, longitude, latitude) ;
        probability:long_name = "probability of presence of iceberg" ;
        probability:units = "1/km2" ;
        probability:valid_min = 0. ;
        probability:valid_max = 1. ;
        probability:_FillValue = 9.96921e+36f ;
        probability:content = "TYX" ;
        probability:associates = "time latitude longitude" ;
    float ice_volume(time, longitude, latitude) ;
        ice_volume:long_name = "volume of ice" ;
        ice_volume:units = "GigaTons" ;
        ice_volume:valid_min = 0. ;
        ice_volume:valid_max = 100. ;
        ice_volume:_FillValue = 9.96921e+36f ;
        ice_volume:content = "TYX" ;
        ice_volume:associates = "time latitude longitude" ;
    float ice_area(time, longitude, latitude) ;
        ice_area:long_name = "mean area of iceberg" ;
        ice_area:units = "km2" ;
        ice_area:valid_min = 0. ;
        ice_area:valid_max = 100. ;
        ice_area:_FillValue = 9.96921e+36f ;
        ice_area:content = "TYX" ;
        ice_area:associates = "time latitude longitude" ;
```

```

float ice_length(longitude , latitude) ;
    ice_length:long_name = "mean length of iceberg from a log normal fit of pd
    ice_length:units = "km" ;
    ice_length:valid_min = 0. ;
    ice_length:valid_max = 2000. ;
    ice_length:_FillValue = 9.96921e+36f ;
    ice_length:content = "YX" ;
    ice_length:associates = "latitude longitude" ;

// global attributes :
    :source = "ENVISAT SGDR" ;
    :project = "Altiberg" ;
    :authors = " J. Tournadre & M. Accensi " ;
    :contact = "cersat@ifremer.fr" ;
    :southernmost_latitude = -90. ;
    :northernmost_latitude = -40. ;
    :latitude_resolution = 1. ;
    :westernmost_longitude = 0. ;
    :easternmost_longitude = 360. ;
    :longitude_resolution = 2. ;
    :start_date = "20110101T000000" ;
    :stop_date = "20111201T000000" ;
    :field_type = "monthly" ;
    :sensor = "envisat" ;
}

```

2.1.2.5 High resolution gridded products

Matlab Gridded products

filename convention prod_gridded_merged_year.mat

- year : four digit year ex : 2010

The polar grid is a regular grid of 50 km x50km or 100x100 km cells from -7000 to +7000 km from the pole.

The lat/lon grid is 1°latitude by 2° longitude from 90°S to 40°S and 0 to 360°E.

Variables

- LAT : Latitudes of the cells
- LON: Longitudes of the cell
- Nicelalo : Biweekly (26) Probability of presence of iceberg on the regular lat/lon grid
- SURFICElalo : Biweekly (26) Mean surface of iceberg on the regular lat/lon grid
- VOLLalo : Biweekly (26) Volume of ice on the regular lat/lon grid
- alat : Latitude of the 100 km regular polar grid
- alon : Longitude of the 100km regular polar grid
- alat50 : Latitude of the 50 km regular polar grid

- alon50 : Longitude of the 50 km regular polar grid
- Nice : Biweekly (26) Probability of presence of iceberg on the regular 100 km polar grid
- Nice50 : Biweekly (26) Probability of presence of iceberg on the regular 50 km polar grid
- SURFICE : Biweekly (26) Mean surface of iceberg on the 100km regular polar grid
- SURFICE50 : Biweekly (26) Mean surface of iceberg on the 50 km regular polar grid
- VOL : Biweekly (26) Volume of ice on the 100km regular polar grid
- VOL50 : Biweekly (26) Volume of ice on the 50km regular polar grid

netcdf files

Three netcdf files are available, a 50 km regular polar grid one, a 100 km regular polar grid one and a 1x1° lat/lon ones.

netcdf filename convention prod_latlon_merged_year.nc
 netcdf filename convention prod_polar50_merged_year.nc
 netcdf filename convention prod_polar100_merged_year.nc
 sat : (*merged,merged_csi*)
 year : four digit year ex : 2010

lat/lon

```
Source:
    prod_latlon_merged_2010.nc
Format:
    netcdf4
Global Attributes:
    source           = 'MERGED SGDR'
    project          = 'Altiberg'
    authors          = ' J. Tournadre & M. Accensi '
    contact          = 'cersat@ifremer.fr'
    southernmost_latitude = -90
    northernmost_latitude = -40
    latitude_resolution = 1
    westernmost_longitude = 0
    easternmost_longitude = 360
    longitude_resolution = 1
    start_date       = '20100101T000000'
    stop_date        = '20101201T000000'
    field_type       = 'monthly'
    sensor           = 'merged'
Dimensions:
    time             = 26
    longitude        = 361
    latitude         = 51
Variables:
    time
        Size:          26x1
        Dimensions:    time
        Datatype:      int32
        Attributes:
            units       = 'days since 1990-01-01T00:00:00Z'
            long_name   = 'julian day (UT)'
            standard_name = 'time'
```

```

        conventions = 'Relative julian days'
        axis        = 'T'
longitude
  Size:          361x1
  Dimensions:   longitude
  Datatype:     double
  Attributes:
    long_name    = 'longitude'
    standard_name = 'longitude'
    units        = 'degree_east'
    valid_min    = '-180'
    valid_max    = '180'
    axis        = 'X'
latitude
  Size:          51x1
  Dimensions:   latitude
  Datatype:     double
  Attributes:
    long_name    = 'latitude'
    standard_name = 'latitude'
    units        = 'degree_north'
    valid_min    = '-90'
    valid_max    = '90'
    axis        = 'Y'
probability
  Size:          51x361x26
  Dimensions:   latitude , longitude , time
  Datatype:     single
  Attributes:
    long_name    = 'probability of presence of iceberg'
    units        = '1/km2'
    valid_min    = 0
    valid_max    = 1
    _FillValue   = 9.969209968386869e+36
    content      = 'TYX'
    associates   = 'time latitude longitude'
ice_volume
  Size:          51x361x26
  Dimensions:   latitude , longitude , time
  Datatype:     single
  Attributes:
    long_name    = 'volume of ice'
    units        = 'GigaTons'
    valid_min    = 0
    valid_max    = 100
    _FillValue   = 9.969209968386869e+36
    content      = 'TYX'
    associates   = 'time latitude longitude'
ice_area
  Size:          51x361x26
  Dimensions:   latitude , longitude , time
  Datatype:     single
  Attributes:
    long_name    = 'mean area of iceberg'
    units        = 'km2'
    valid_min    = 0
    valid_max    = 100
    _FillValue   = 9.969209968386869e+36
    content      = 'TYX'
    associates   = 'time latitude longitude'
ice_length
  Size:          51x361
  Dimensions:   latitude , longitude
  Datatype:     single
  Attributes:
    long_name    = 'mean length of iceberg from a log normal fit of pdf'
    units        = 'km'
    valid_min    = 0
    valid_max    = 2000

```

```

    _FillValue = 9.969209968386869e+36
    content    = 'YX'
    associates = 'latitude longitude'

```

Polar

```

netcdf4
Global Attributes:
  source      = 'MERGED SGDR'
  project     = 'Altiberg'
  authors     = 'J. Tournadre & M. Accensi'
  contact     = 'cersat@ifremer.fr'
  southernmost_latitude = -90
  northernmost_latitude = 11.8035
  latitude_resolution = 'n/a'
  westernmost_longitude = -179.5908
  easternmost_longitude = 180
  longitude_resolution = 'n/a'
  start_date  = '20100101T000000'
  stop_date   = '20101201T000000'
  field_type  = 'monthly'
  sensor      = 'merged'

Dimensions:
  time        = 26
  Lambert X coordinate = 281
  Lambert Y coordinate = 281

Variables:
  time
    Size:      26x1
    Dimensions: time
    Datatype:  int32
    Attributes:
      units      = 'days since 1990-01-01T00:00:00Z'
      long_name  = 'julian day (UT)'
      standard_name = 'time'
      conventions = 'Relative julian days'
      axis      = 'T'

  x
    Size:      281x1
    Dimensions: Lambert X coordinate
    Datatype:  double
    Attributes:
      long_name  = 'X coordinate in south polar Lambert projection'
      standard_name = 'projection_x_coordinate'
      units      = 'km'
      valid_min  = '-7000'
      valid_max  = '7000'
      axis      = 'X'

  y
    Size:      281x1
    Dimensions: Lambert Y coordinate
    Datatype:  double
    Attributes:
      long_name  = 'Y coordinate in south polar Lambert projection'
      standard_name = 'projection_y_coordinate'
      units      = 'km'
      valid_min  = '-7000'
      valid_max  = '7000'
      axis      = 'Y'

  probability
    Size:      281x281x26
    Dimensions: Lambert X coordinate, Lambert Y coordinate, time
    Datatype:  single
    Attributes:
      long_name  = 'iceberg probability'
      units      = '1/km2'
      valid_min  = 0
      valid_max  = 1
      _FillValue = 9.969209968386869e+36
      content    = 'TYX'
      associates = 'time latitude longitude'

  ice_volume
    Size:      281x281x26
    Dimensions: Lambert X coordinate, Lambert Y coordinate, time
    Datatype:  single
    Attributes:
      long_name  = 'volume of ice'
      units      = 'GigaTons'
      valid_min  = 0
      valid_max  = 100
      _FillValue = 9.969209968386869e+36
      content    = 'TYX'
      associates = 'time latitude longitude'

  ice_area
    Size:      281x281x26
    Dimensions: Lambert X coordinate, Lambert Y coordinate, time
    Datatype:  single

```

```

Attributes :
    long_name = 'mean area of iceberg '
    units     = 'km2'
    valid_min = 0
    valid_max = 100
    _FillValue = 9.969209968386869e+36
    content   = 'TYX'
    associates = 'time latitude longitude '

latitude
Size:      281x281
Dimensions: Lambert X coordinate ,Lambert Y coordinate
Datatype:  single
Attributes:
    long_name     = 'latitude of grid points '
    standard_name = 'latitude '
    sensor        = 'merged'
    units         = 'degree_north '
    valid_min     = -90
    valid_max     = 90
    _FillValue    = 9.969209968386869e+36
    content       = 'TYX'
    associates    = 'time latitude longitude '

longitude
Size:      281x281
Dimensions: Lambert X coordinate ,Lambert Y coordinate
Datatype:  single
Attributes:
    long_name     = 'longitude of grid points '
    standard_name = 'longitude '
    units         = 'degree_east '
    valid_min     = -180
    valid_max     = 180
    _FillValue    = 9.969209968386869e+36
    content       = 'TYX'
    associates    = 'time longitude longitude '

```

2.2 Arctic data set

2.2.1 Matlab files

2.2.1.1 Individual iceberg files

filename convention: *iceberg_sat_year1year2.mat*

- *sat* : (*ers1,ers2,topex, envisat, Jason1, Jason1b, Jason2,Jason3, Cryosat, Cryosat-SAR, altika, HY2A, HY2CNES, sentinel3A, sentinel3ALRM, HY2B, merged*)
- *year1year2*: *year1=beginning year, year2: end year*

Variables

- *ic_anne* year
- *ic_mois* month
- *ic_jour* day
- *ic_Tjul* time in julian day (*matlab format*)
- *ic_CYCL* satellite cycle number
- *ic_TR* satellite track number
- *ic_lat* latitude
- *ic_lon* longitude (*0 360°*)

- *ic_LambX* polar Lambert coordinates X
- *ic_LambY* : polar Lambert coordinates Y
- *ic_Jecho* Position of the echo : range bin of the echo (from convolution)
- *ic_Jk* Position of the echo : range bin of the echo (from waveforms)
- *ic_conc* Sea ice concentration from monthly mean SSMI fields (%)
- *ic_sig* Iceberg backscatter (dB)
- *ic_sig_cal* Calibrated Iceberg backscatter (dB)
- *ic_surf* Iceberg area (km²)
- *ic_surf_cal* Calibrated Iceberg area (km²)
- *ic_di* Distance from nadir (km)
- *ic_di_cal* Calibrated Distance from nadir (km)
- *ic_sat* satellite that detected the iceberg (**for merged files only**)
- *ic_sat* satellite that detected the iceberg (**for merged files only**), ers1, 2 ers2; 3 topex; 4 Jason1; 5 Jason2; 6 Jason1b; 7 Cryosat; 8 envisat; 9 Altika, 10 HY2A; 11 HY2ACNES, 12 Jason3; 13 CryosatSAR; 14 Sentinel3ALRM; 15 Sentinel3BLRM; 16 Cryosat; 17 Cryosat-sarin

2.2.1.2 Gridded products

filename convention prod_gridded_sat_year1-year2.mat

- *sat* : (*ers1,ers2,topex, envisat, Jason1, Jason1b, Jason2,Jason3, Cryosat, Cryosat-SAR, altika, HY2A, HY2CNES, sentinel3A, sentinel3ALRM, merged*)
- *year1year2*: *year1=beginning year, year2: end year* : (1992-2020)

The polar grid is a regular grid of 50 km x50km cells from -7000 to +7000 km from the pole. The lat/lon grid is 1°latitude by 2° longitude from 5°N to 80°N and -180 to 180°E.

All the fields are 4 dimensional X(i,j,k,l) i and j are the grid cell indices, k is the year (1=1992) and l the month.

Variables

- LAT : Latitudes of the cells
- LON: Longitudes of the cell
- Nicelalo : yearly and Monthly (12) Probability of presence of iceberg on the regular lat/lon grid
- SURFICelalo : Monthly (12) Mean surface of iceberg on the regular lat/lon grid
- VOLlalo : Monthly (12) Volume of ice on the regular lat/lon grid

- `alat` : Latitude of the regular polar grid
- `alon` : Longitude of the regular polar grid
- `Nice` : Monthly (12) Probability of presence of iceberg on the regular polar grid
- `SURFICElalo` : Monthly (12) Mean surface of iceberg on the regular polar grid
- `VOLLalo` : Monthly (12) Volume of ice on the regular polar grid
- `surf_norm` : surface of the altimeter swath (km²) (*set to 0 for merged products*)

2.2.2 Netcdf files

2.2.2.1 Individual iceberg files

netcdf filename convention: `iceberg_sat_year.nc`

- `sat` : (*ers1,ers2,topex, envisat, Jason1, Jason1b, Jason2,Jason3, Cryosat, Cryosat-SAR, altika, HY2A, HY2CNES, sentinel3A, sentinel3ALRM, HY2B, merged*)
- `year` : four digit year ex : 2001

```
netcdf iceberg_jason3_20162019 {
dimensions:
    time = 1437 ;
variables:
    int time(time) ;
        time:units = "days since 1990-01-01T00:00:00Z" ;
        time:long_name = "julian day (UT)" ;
        time:standard_name = "time" ;
        time:conventions = "Relative julian days" ;
        time:axis = "T" ;
    float lat(time) ;
        lat:long_name = "latitude" ;
        lat:standard_name = "latitude" ;
        lat:units = "degree_north" ;
        lat:valid_min = -90. ;
        lat:valid_max = 90. ;
        lat:_FillValue = 9.96921e+36f ;
        lat:content = "T" ;
        lat:associates = "time" ;
    float lon(time) ;
        lon:long_name = "longitude" ;
        lon:standard_name = "longitude" ;
        lon:units = "degree_east" ;
        lon:valid_min = -180. ;
        lon:valid_max = 180. ;
        lon:_FillValue = 9.96921e+36f ;
        lon:content = "T" ;
        lon:associates = "time" ;
```



```
float lambx(time) ;
    lambx:long_name = "x coordinate in lambert south pole projection" ;
    lambx:standard_name = "projection_x_coordinate" ;
    lambx:units = "km" ;
    lambx:valid_min = 0. ;
    lambx:valid_max = 10000. ;
    lambx:_FillValue = 9.96921e+36f ;
    lambx:content = "T" ;
    lambx:associates = "time" ;
float lamby(time) ;
    lamby:long_name = "y coordinate in lambert south pole projection" ;
    lamby:standard_name = "projection_y_coordinate" ;
    lamby:units = "km" ;
    lamby:valid_min = 0. ;
    lamby:valid_max = 100. ;
    lamby:_FillValue = 9.96921e+36f ;
    lamby:content = "T" ;
    lamby:associates = "time" ;
float cycle(time) ;
    cycle:long_name = "satellite cycle number" ;
    cycle:units = "n/a" ;
    cycle:valid_min = 0. ;
    cycle:valid_max = 1000. ;
    cycle:_FillValue = 9.96921e+36f ;
    cycle:content = "T" ;
    cycle:associates = "time" ;
float pass_number(time) ;
    pass_number:long_name = "satellite pass number" ;
    pass_number:units = "n/a" ;
    pass_number:valid_min = 0. ;
    pass_number:valid_max = 100. ;
    pass_number:_FillValue = 9.96921e+36f ;
    pass_number:content = "T" ;
    pass_number:associates = "time" ;
float j_conv(time) ;
    j_conv:long_name = "range bin of the iceberg echo (convolution)" ;
    j_conv:units = "n/a" ;
    j_conv:valid_min = 0. ;
    j_conv:valid_max = 100. ;
    j_conv:_FillValue = 9.96921e+36f ;
    j_conv:content = "T" ;
    j_conv:associates = "time" ;
float j_wf(time) ;
    j_wf:long_name = "range bin of the iceberg echo (waveform)" ;
    j_wf:units = "n/a" ;
    j_wf:valid_min = 0. ;
    j_wf:valid_max = 100. ;
    j_wf:_FillValue = 9.96921e+36f ;
    j_wf:content = "T" ;
    j_wf:associates = "time" ;
float sigma0(time) ;
    sigma0:long_name = "iceberg backscatter at Ku band" ;
    sigma0:units = "dB" ;
    sigma0:valid_min = 0. ;
    sigma0:valid_max = 100. ;
```

```

        sigma0:_FillValue = 9.96921e+36f ;
        sigma0:content = "T" ;
        sigma0:associates = "time" ;
float surface(time) ;
        surface:long_name = "iceberg surface" ;
        surface:units = "km2" ;
        surface:valid_min = 0. ;
        surface:valid_max = 1000. ;
        surface:_FillValue = 9.96921e+36f ;
        surface:content = "T" ;
        surface:associates = "time" ;
float distance(time) ;
        distance:long_name = "distance of the iceberg from nadir" ;
        distance:units = "km" ;
        distance:valid_min = 0. ;
        distance:valid_max = 100. ;
        distance:_FillValue = 9.96921e+36f ;
        distance:content = "T" ;
        distance:associates = "time" ;
float sigma0_cal(time) ;
        sigma0_cal:long_name = "iceberg backscatter at Ku band calibrated" ;
        sigma0_cal:units = "dB" ;
        sigma0_cal:valid_min = 0. ;
        sigma0_cal:valid_max = 100. ;
        sigma0_cal:_FillValue = 9.96921e+36f ;
        sigma0_cal:content = "T" ;
        sigma0_cal:associates = "time" ;
float surface_cal(time) ;
        surface_cal:long_name = "iceberg surface from calibrated backscatter" ;
        surface_cal:units = "km2" ;
        surface_cal:valid_min = 0. ;
        surface_cal:valid_max = 100. ;
        surface_cal:_FillValue = 9.96921e+36f ;
        surface_cal:content = "T" ;
        surface_cal:associates = "time" ;
float distance_cal(time) ;
        distance_cal:long_name = "distance of the iceberg from nadir using the cal
        distance_cal:units = "db" ;
        distance_cal:valid_min = 0. ;
        distance_cal:valid_max = 100. ;
        distance_cal:_FillValue = 9.96921e+36f ;
        distance_cal:content = "T" ;
        distance_cal:associates = "time" ;
float sea_ice_conc(time) ;
        sea_ice_conc:long_name = " Daily sea ice concentration from SSMI" ;
        sea_ice_conc:standard_name = "sea_ice_area_fraction" ;
        sea_ice_conc:units = "%" ;
        sea_ice_conc:valid_min = 0. ;
        sea_ice_conc:valid_max = 100. ;
        sea_ice_conc:_FillValue = 9.96921e+36f ;
        sea_ice_conc:content = "T" ;
        sea_ice_conc:associates = "time" ;

// global attributes :
        :source = "JASON3 SGDR" ;

```

```

:project = "Altiberg " ;
:authors = "J. Tournadre & M. Accensi" ;
:contact = "cersat@ifremer.fr" ;
:start_date = "20160101T000000" ;
:stop_date = "20190101T000000" ;
:field_type = "yearly" ;
:sensor = "jason3" ;
}

```

2.2.2.2 Merged iceberg files

netcdf filename convention: iceberg_sat_year.nc

- o *sat* : (**merged**)

- o *year* : four digit year ex : 2001

```

netcdf iceberg_merged_19922019 {
dimensions:
    time = 47816 ;
variables:
    int time(time) ;
        time:units = "days since 1990-01-01T00:00:00Z" ;
        time:long_name = "julian day (UT)" ;
        time:standard_name = "time" ;
        time:conventions = "Relative julian days" ;
        time:axis = "T" ;
    float lat(time) ;
        lat:long_name = "latitude" ;
        lat:standard_name = "latitude" ;
        lat:units = "degree_north" ;
        lat:valid_min = -90. ;
        lat:valid_max = 90. ;
        lat:_FillValue = 9.96921e+36f ;
        lat:content = "T" ;
        lat:associates = "time" ;
    float lon(time) ;
        lon:long_name = "longitude" ;
        lon:standard_name = "longitude" ;
        lon:units = "degree_east" ;
        lon:valid_min = -180. ;
        lon:valid_max = 180. ;
        lon:_FillValue = 9.96921e+36f ;
        lon:content = "T" ;
        lon:associates = "time" ;
    float lambx(time) ;
        lambx:long_name = "x coordinate in lambert south pole projection" ;
        lambx:standard_name = "projection_x_coordinate" ;
        lambx:units = "km" ;
        lambx:valid_min = 0. ;
        lambx:valid_max = 10000. ;
        lambx:_FillValue = 9.96921e+36f ;
        lambx:content = "T" ;
        lambx:associates = "time" ;
    float lamby(time) ;

```

```

        lamby:long_name = "y coordinate in lambert south pole projection" ;
        lamby:standard_name = "projection_y_coordinate" ;
        lamby:units = "km" ;
        lamby:valid_min = 0. ;
        lamby:valid_max = 100. ;
        lamby:_FillValue = 9.96921e+36f ;
        lamby:content = "T" ;
        lamby:associates = "time" ;
float cycle(time) ;
        cycle:long_name = "satellite cycle number" ;
        cycle:units = "n/a" ;
        cycle:valid_min = 0. ;
        cycle:valid_max = 1000. ;
        cycle:_FillValue = 9.96921e+36f ;
        cycle:content = "T" ;
        cycle:associates = "time" ;
float pass_number(time) ;
        pass_number:long_name = "satellite pass number" ;
        pass_number:units = "n/a" ;
        pass_number:valid_min = 0. ;
        pass_number:valid_max = 100. ;
        pass_number:_FillValue = 9.96921e+36f ;
        pass_number:content = "T" ;
        pass_number:associates = "time" ;
float j_conv(time) ;
        j_conv:long_name = "range bin of the iceberg echo (convolution)" ;
        j_conv:units = "n/a" ;
        j_conv:valid_min = 0. ;
        j_conv:valid_max = 100. ;
        j_conv:_FillValue = 9.96921e+36f ;
        j_conv:content = "T" ;
        j_conv:associates = "time" ;
float j_wf(time) ;
        j_wf:long_name = "range bin of the iceberg echo (waveform)" ;
        j_wf:units = "n/a" ;
        j_wf:valid_min = 0. ;
        j_wf:valid_max = 100. ;
        j_wf:_FillValue = 9.96921e+36f ;
        j_wf:content = "T" ;
        j_wf:associates = "time" ;
float sigma0(time) ;
        sigma0:long_name = "iceberg backscatter at Ku band" ;
        sigma0:units = "dB" ;
        sigma0:valid_min = 0. ;
        sigma0:valid_max = 100. ;
        sigma0:_FillValue = 9.96921e+36f ;
        sigma0:content = "T" ;
        sigma0:associates = "time" ;
float surface(time) ;
        surface:long_name = "iceberg surface" ;
        surface:units = "km2" ;
        surface:valid_min = 0. ;
        surface:valid_max = 1000. ;
        surface:_FillValue = 9.96921e+36f ;
        surface:content = "T" ;

```

```

        surface:associates = "time" ;
float distance(time) ;
        distance:long_name = "distance of the iceberg from nadir" ;
        distance:units = "km" ;
        distance:valid_min = 0. ;
        distance:valid_max = 100. ;
        distance:_FillValue = 9.96921e+36f ;
        distance:content = "T" ;
        distance:associates = "time" ;
float sigma0_cal(time) ;
        sigma0_cal:long_name = "iceberg backscatter at Ku band calibrated"
        sigma0_cal:units = "dB" ;
        sigma0_cal:valid_min = 0. ;
        sigma0_cal:valid_max = 100. ;
        sigma0_cal:_FillValue = 9.96921e+36f ;
        sigma0_cal:content = "T" ;
        sigma0_cal:associates = "time" ;
float surface_cal(time) ;
        surface_cal:long_name = "iceberg surface from calibrated backscatte
        surface_cal:units = "km2" ;
        surface_cal:valid_min = 0. ;
        surface_cal:valid_max = 100. ;
        surface_cal:_FillValue = 9.96921e+36f ;
        surface_cal:content = "T" ;
        surface_cal:associates = "time" ;
float distance_cal(time) ;
        distance_cal:long_name = "distance of the iceberg from nadir using
        distance_cal:units = "db" ;
        distance_cal:valid_min = 0. ;
        distance_cal:valid_max = 100. ;
        distance_cal:_FillValue = 9.96921e+36f ;
        distance_cal:content = "T" ;
        distance_cal:associates = "time" ;
float sea_ice_conc(time) ;
        sea_ice_conc:long_name = " Daily sea ice concentration from SSML" ;
        sea_ice_conc:standard_name = "sea_ice_area_fraction" ;
        sea_ice_conc:units = "%" ;
        sea_ice_conc:valid_min = 0. ;
        sea_ice_conc:valid_max = 100. ;
        sea_ice_conc:_FillValue = 9.96921e+36f ;
        sea_ice_conc:content = "T" ;
        sea_ice_conc:associates = "time" ;
float sat(time) ;
        sat:long_name = "satellite that detected the iceberg, 1 ers1, 2 ers
        sat:standard_name = "satellite" ;
        sat:units = "-" ;
        sat:scale_factor = 1. ;
        sat:valid_max = 8. ;
        sat:_FillValue = 9.96921e+36f ;
        sat:content = "T" ;
        sat:associates = "time" ;

// global attributes :
        :source = "MERGED SGDR" ;
        :project = "Altiberg " ;

```

```
    :authors = "J. Tournadre & M. Accensi" ;  
    :contact = "cersat@ifremer.fr" ;  
    :start_date = "19910101T000000" ;  
    :stop_date = "20190101T000000" ;  
    :field_type = "yearly" ;  
    :sensor = "merged" ;  
}
```

Annex

Antarctic mean merged annual ice volume fields

Antarctic mean merged HR annual ice volume fields

Arctic mean merged annual ice volume fields

Contact:

For more information or to report any problem: cersat@ifremer.fr

The data are available on the CERSAT web site : <ftp://ftp.ifremer.fr/ifremer/cersat/projects/altiberg/v3>
and through the CERSAT catalogue <http://cersat.ifremer.fr/data/products/catalogue/> , project
and ALTIBERG

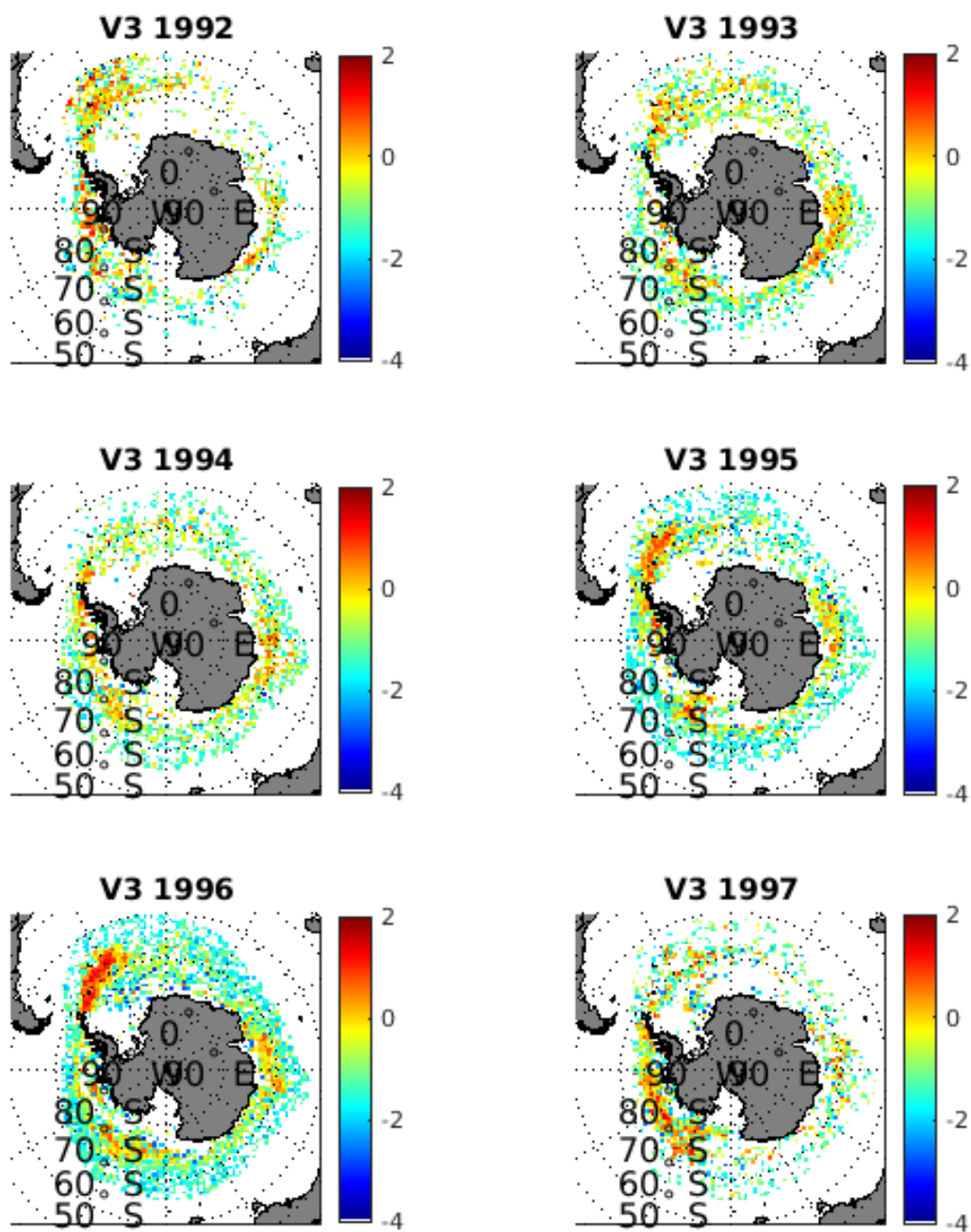


Figure 2.1: Annual merged volume of ice from 1992 to 1996.

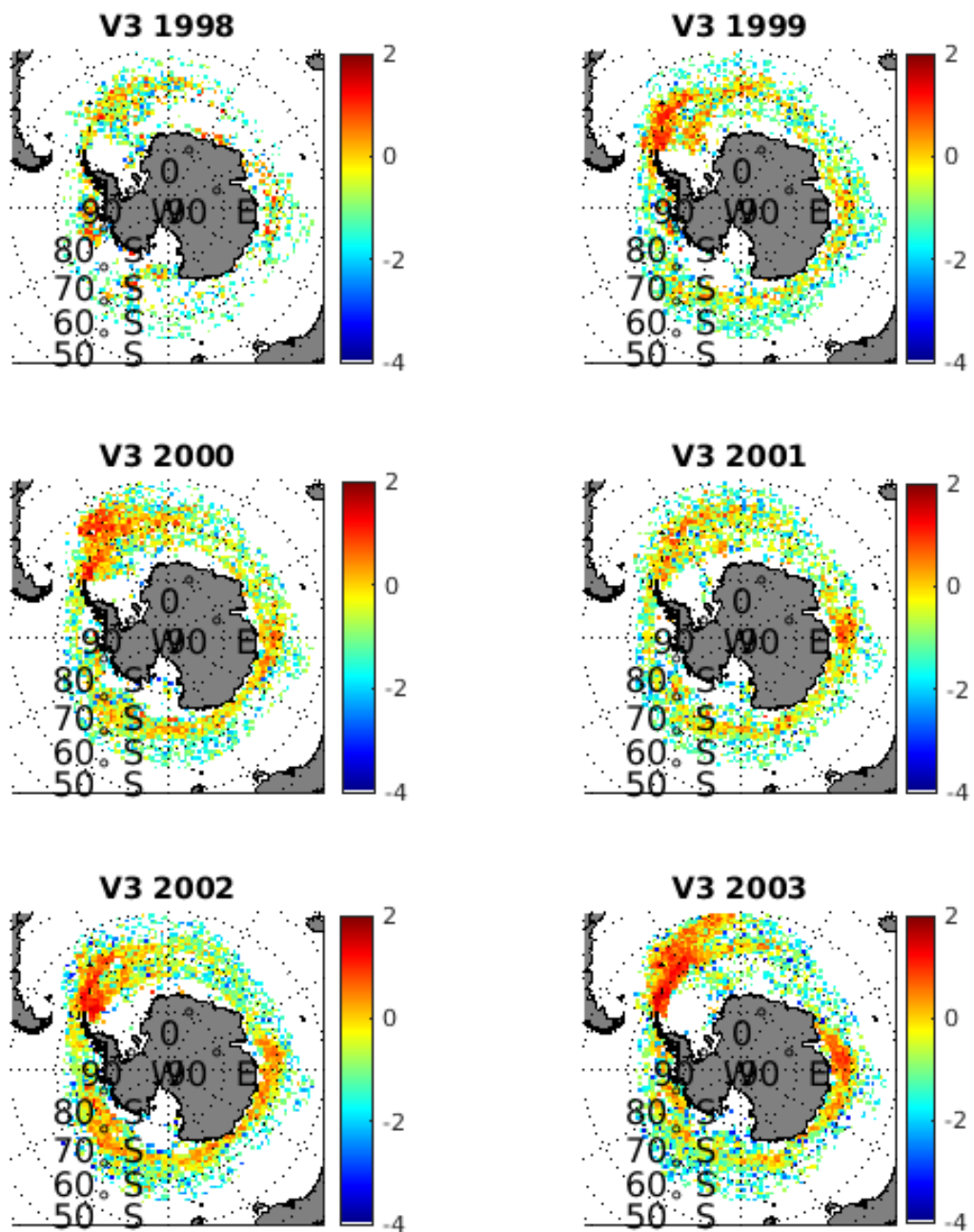


Figure 2.2: Annual merged volume of ice from 1997 to 2002.

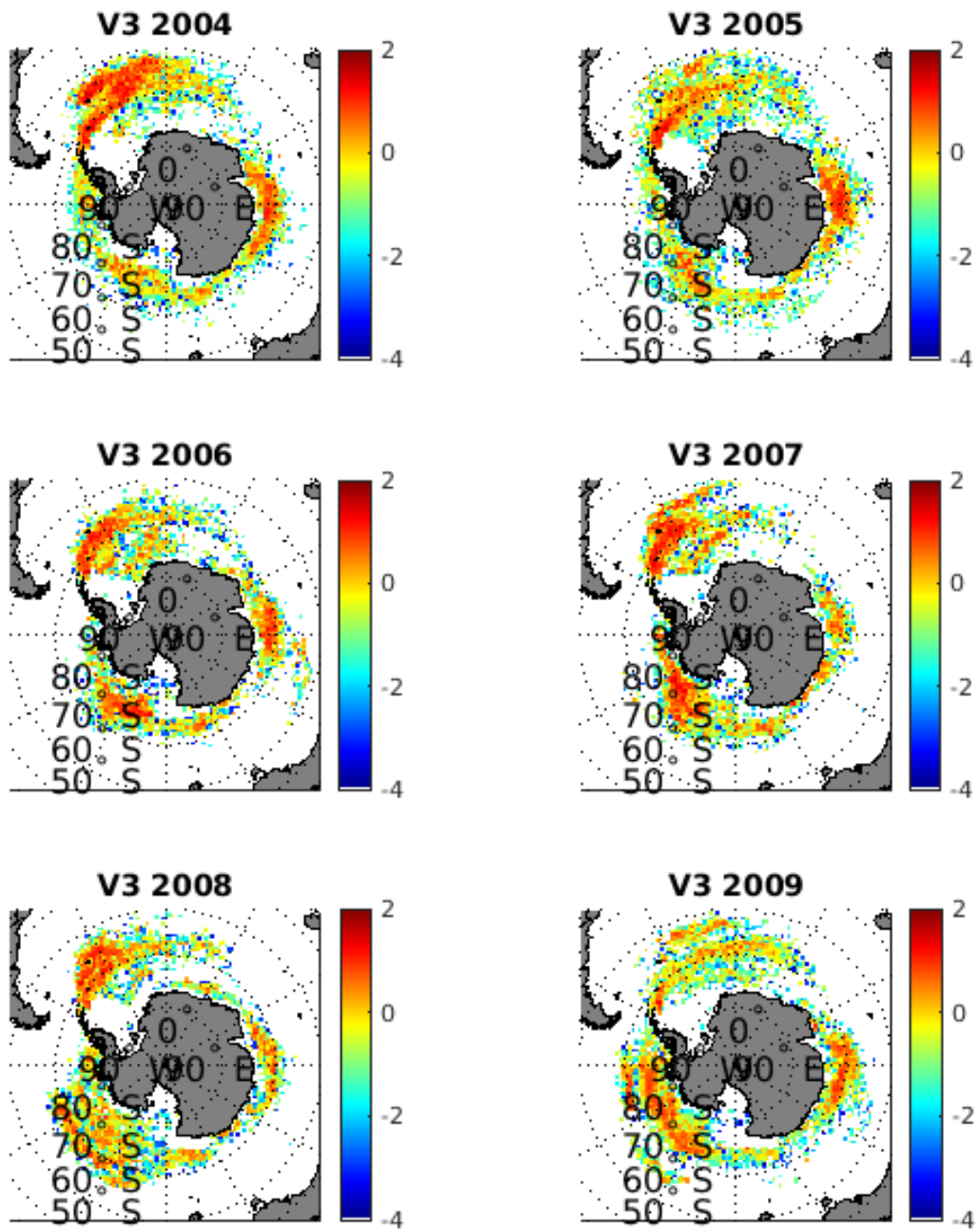


Figure 2.3: Annual merged volume of ice from 2003 to 2008.

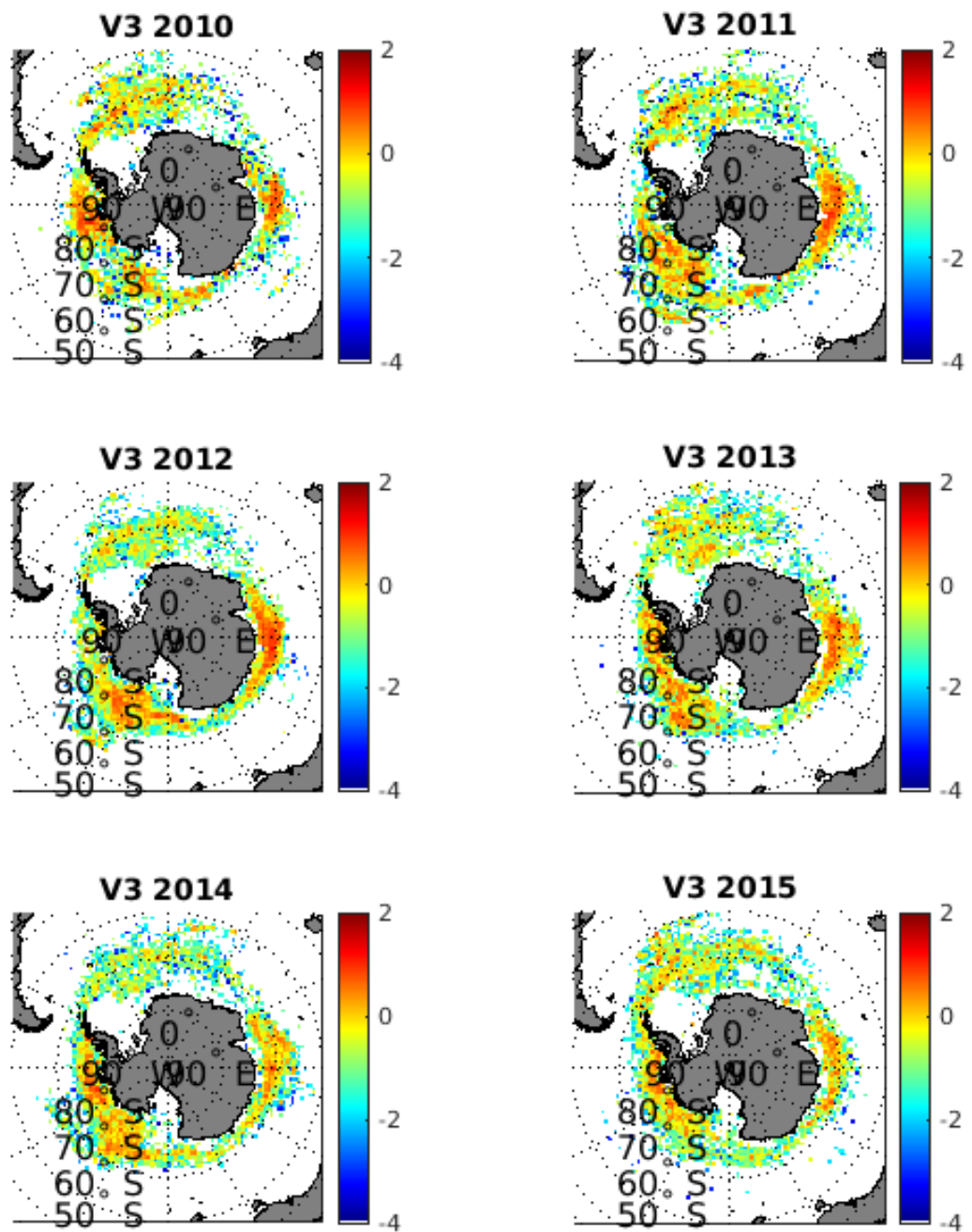


Figure 2.4: Annual merged volume of ice from 2009 to 2014.

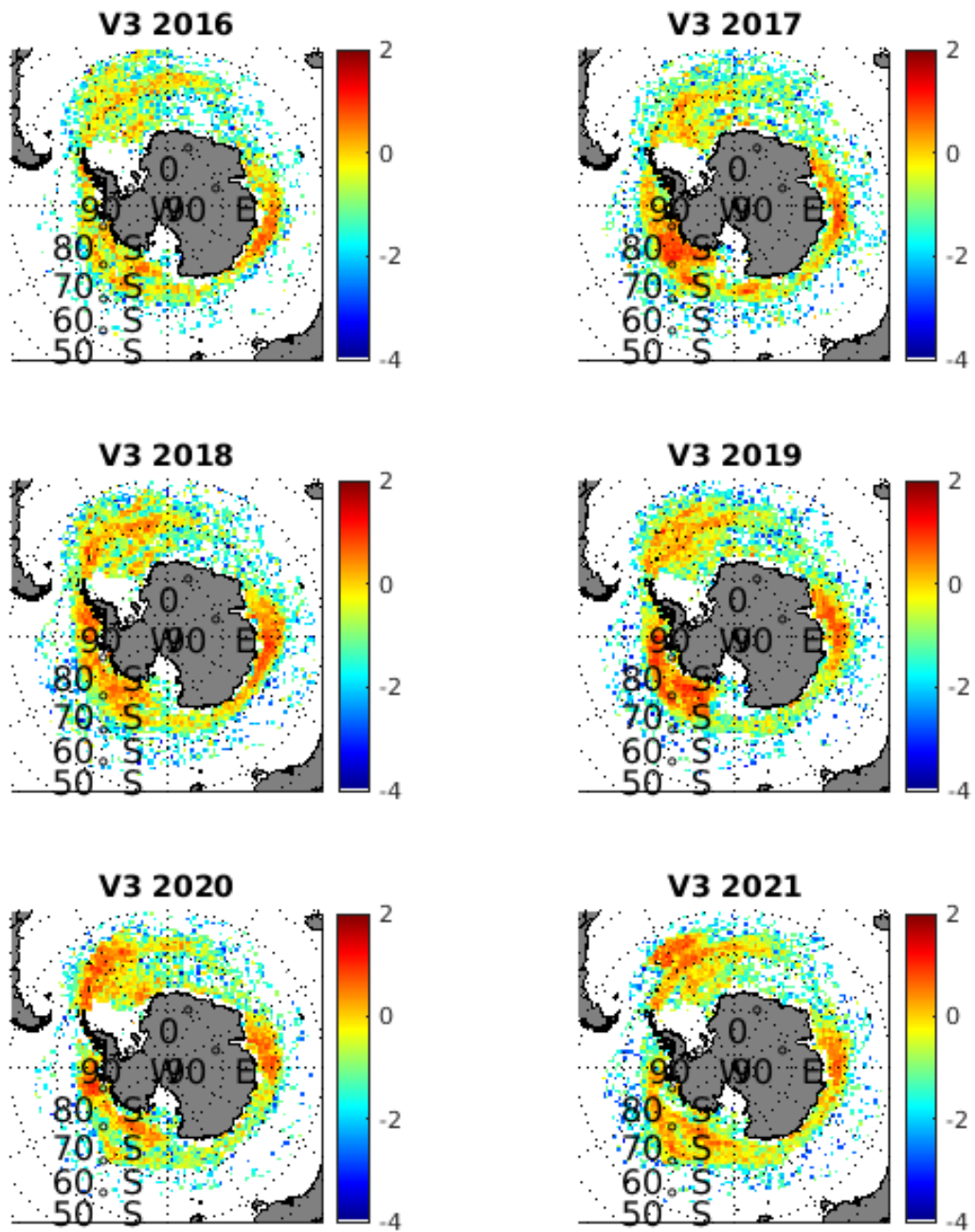


Figure 2.5: Annual merged volume of ice from 2015 to 2021.

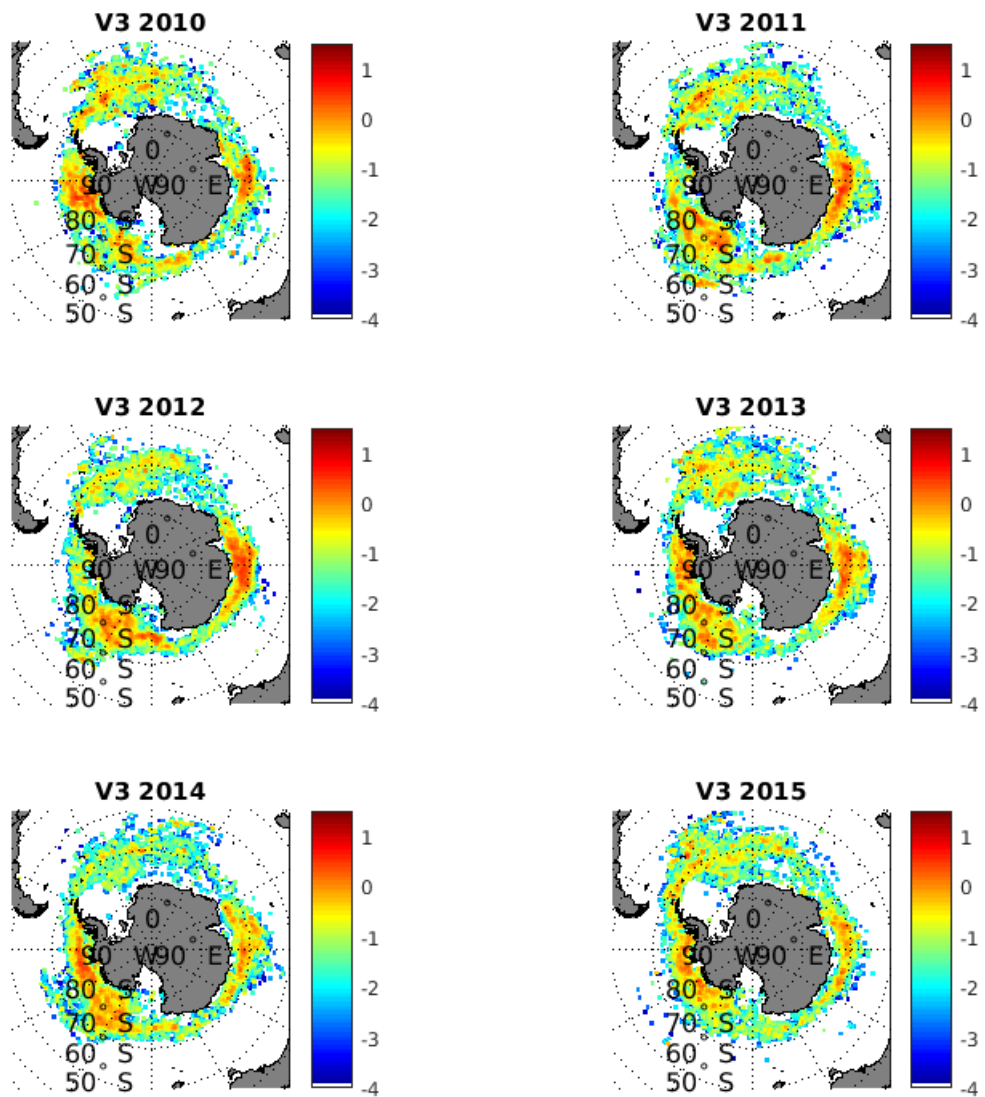


Figure 2.6: Annual merged volume of ice from 2015 to 2020

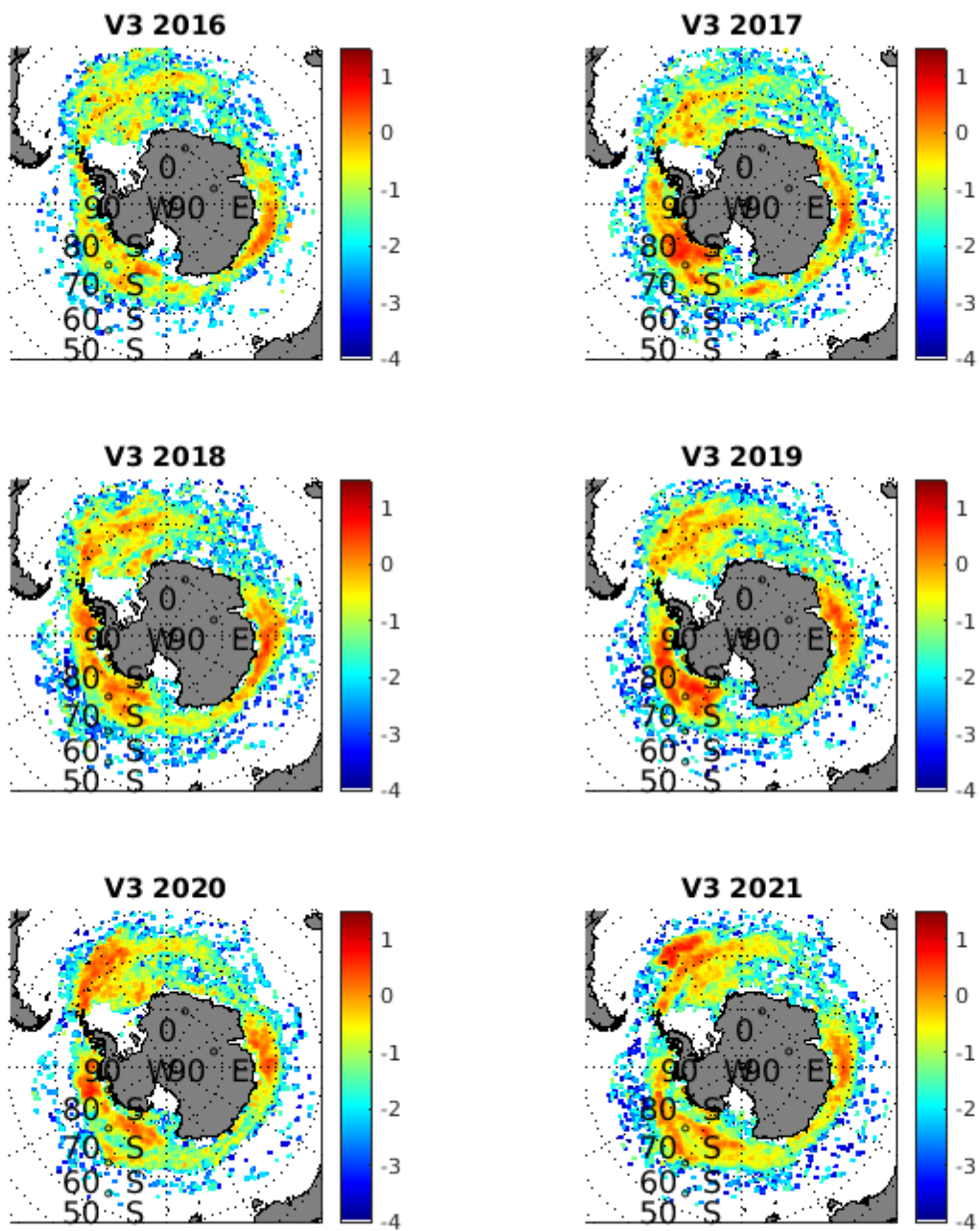


Figure 2.7: Annual merged volume of ice from 2015 to 2020

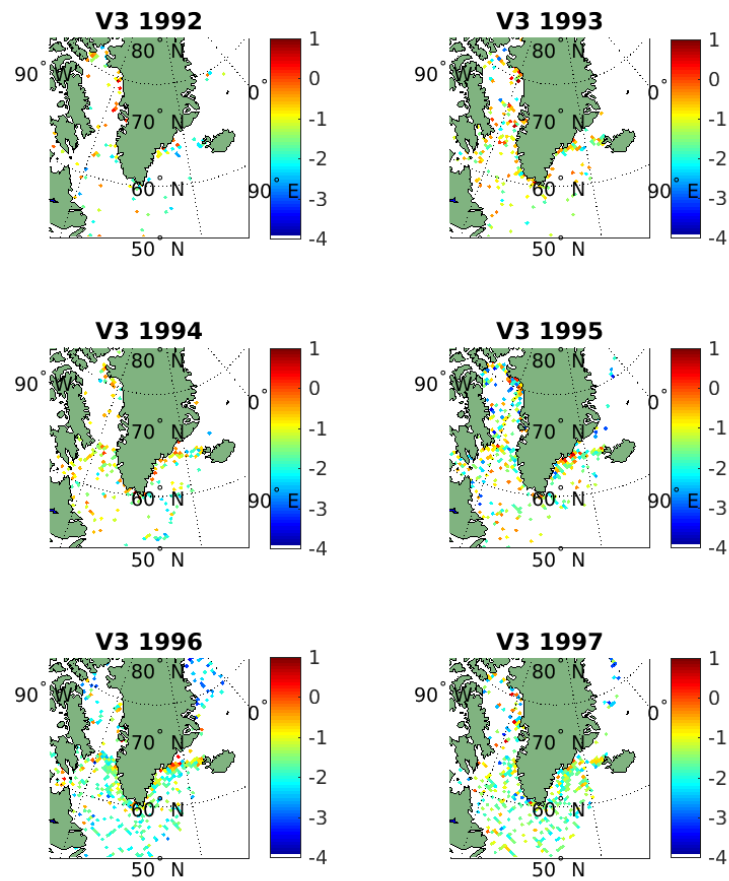


Figure 2.8: Arctic Annual merged volume of ice from 1992 to 1997

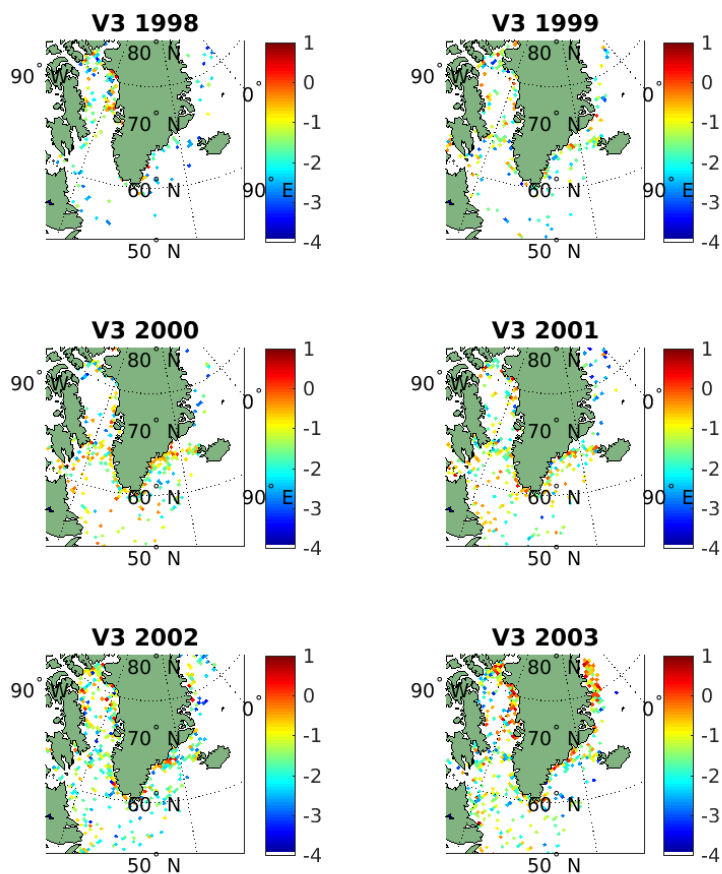


Figure 2.9: Arctic Annual merged volume of ice from 1998 to 2003

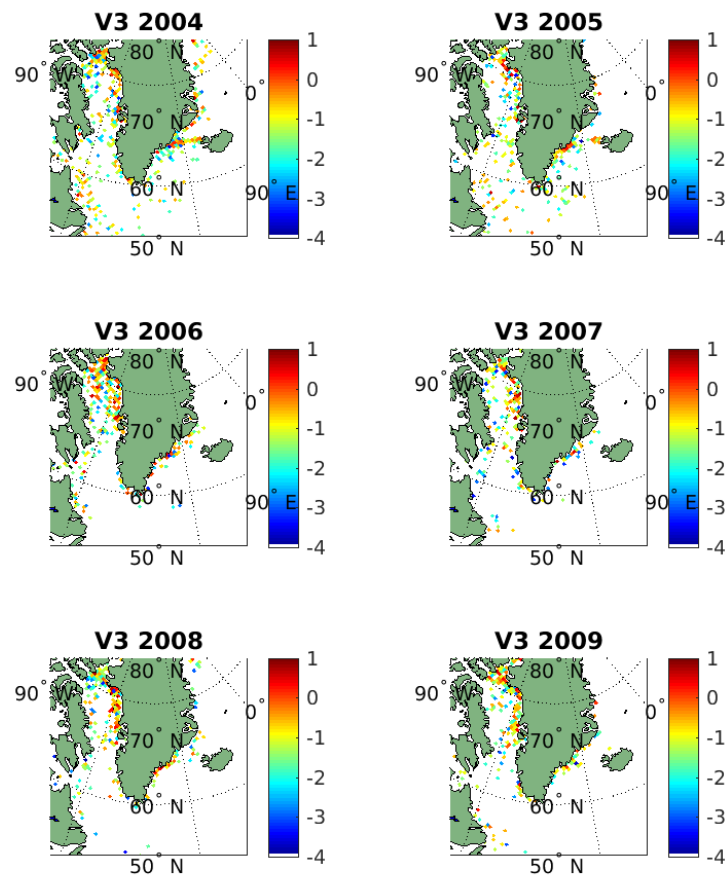


Figure 2.10: Arctic Annual merged volume of ice from 2004 to 2009

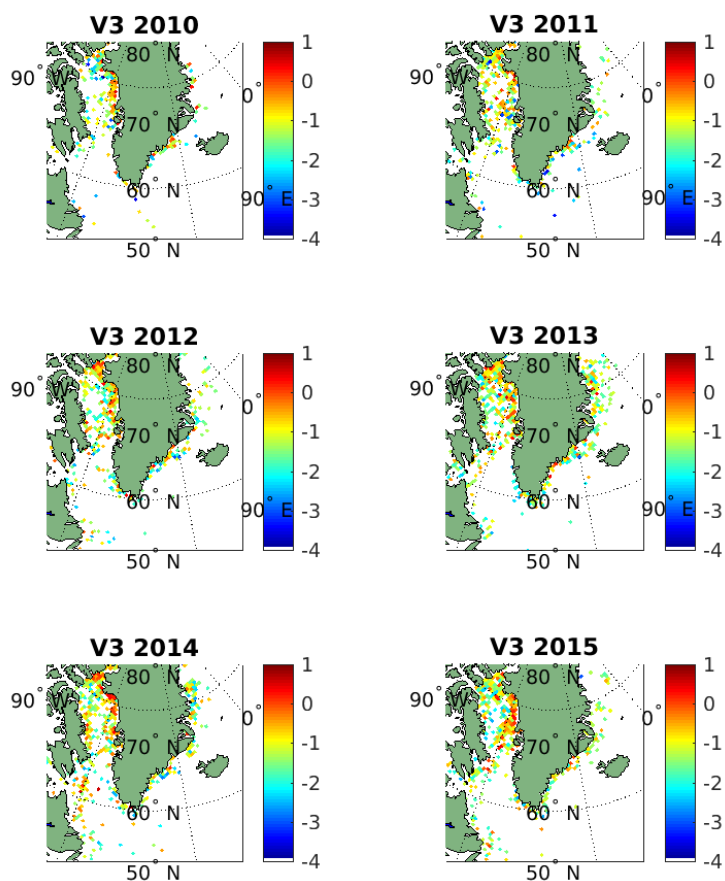


Figure 2.11: Arctic Annual merged volume of ice from 2010 to 2015

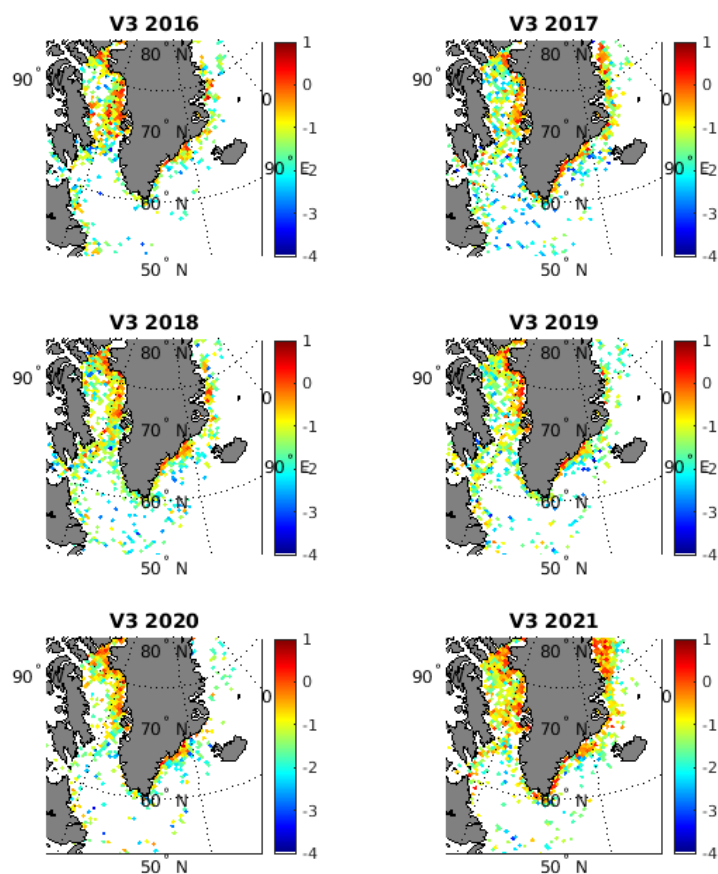


Figure 2.12: Arctic Annual merged volume of ice from 2016 to 2021

Bibliography

- D.E. Barrick and B.J. Lipa. Analysis and interpretation of altimeter sea echo. *Satellite Oceanic Remote Sensing, Adv. Geophysics*, 27:61–100, 1985.
- G. S. Brown. The average impulse response of a rough surface and its applications. *IEEE Trans. Antennas Propag.*, AP-25:67–74, 1977.
- N. Galin, D. J. Wingham, R. Cullen, M. Fornari, W. H. F. Smith, and S. Abdalla. Calibration of the Cryosat-2 interferometer and measurement of across-track ocean slope. *IEEE Trans. Geoscienc. Remote Sens.*, 51(1):57–72, Jan 2013. ISSN 0196-2892. doi: 10.1109/TGRS.2012.2200298.
- R. M. Gladstone, G. R. Bigg, and K. W. Nicholls. Iceberg trajectory modeling and melt-water injection in the Southern Ocean. *J. Geophys. Res.*, 106:19903–19916, 2001. doi: 10.1029/2000JC000347.
- J.R. Jensen. Angle measurement with a phase monopulse radar altimeter. *IEEE Trans. Antennas Propag.*, 47(4):715–724, Apr 1999. ISSN 0018-926X. doi: 10.1109/8.768812.
- B. Legresy, F. Papa, F. Remy, G. Vinay, Mathias Van den Bosch, and O-Z. Zanife. Envisat radar altimeter measurements over continental surfaces and ice caps using the ICE-2 retracking algorithm. *Remote Sens. Environ.*, 95:150–163, 2005.
- S. Nanda. Multiple scatterer retracking and interferometric swath processing of CryoSat-2 data for ice sheet elevation changes. Master's thesis, Dpt. Geoscience & Remote Sensing, Fac. Civil Engineering and Geosciences, Technical University Delft, The Netherlands, 2015.
- R. J. Powell, A. R. Birks, W. J. Wrench, and C. L. Biddiscombe. Using transponders with ERS1-1 and Topex altimeters to measure orbit altitude to ± 3 cm. In *Proc. First ERS- Symposium (ESA SP-359)*, pages 511–516, 1993.
- M. Roca, H. Jackson, and C. Celani. RA-2 sigma-0 absolute calibration. In *Proc. Envisat Validation Workshop (ESA SP-531)*, page 16 pp, 2003.
- Y.A. Romanov, N. A. Romanova, and P. Romanov. Shape and size of Antarctic icebergs derived from ship observation data. *Antarctic Science*, 24:77–87, 2012. doi: 10.1017/S0954102011000538.
- J. Tournadre, K. Whitmer, and F. Girard-Ardhuin. Iceberg detection in open water by altimeter waveform analysis. *J. Geophys. Res.*, 113(C8):C08040, AUG 23 2008. ISSN 0148-0227. doi: 10.1029/2007JC004587.

- J. Tournadre, F. Girard-Ardhuin, and B. Legresy. Antarctic icebergs distributions, 2002-2010. *J. Geophys. Res.*, 117:C05004, MAY 1 2012. ISSN 0148-0227. doi: 10.1029/2011JC007441.
- J. Tournadre, N. Bouhier, F. Girard-Ardhuin, and F. Rémy. Antarctic icebergs distributions 1992-2014. *J. Geophys. Res.*, 121(1):327–349, JAN 2016. ISSN 2169-9275. doi: 10.1002/2015JC011178.
- J. Tournadre, N. Bouhier, F. Boy, and S. Dinardo. Detection of iceberg using delay doppler and interferometric cryosat-2 altimeter data. *Remote Sens. Envir.*, 212:134 – 147, 2018a. ISSN 0034-4257. doi: <https://doi.org/10.1016/j.rse.2018.04.037>. URL <http://www.sciencedirect.com/science/article/pii/S0034425718301949>.
- Jean Tournadre, M. Accensi, and F. Girard-Ardhuin. The altiberg iceberg data base. Tech. Rep. LOS 2013-01, IFREMER, BP 70, 29280, PLouzane, France, 2013.
- Jean Tournadre, M. Accensi, and F. Girard-Ardhuin. The altiberg iceberg data base version-1. Tech. Rep. LOS 2015-01, IFREMER, BP 70, 29280, PLouzane, France, 2015.
- Jean Tournadre, M. Accensi, and F. Girard-Ardhuin. The altiberg iceberg data base: version 2. Tech. Rep. LOS 2017-01, IFREMER, BP 70, 29280, PLouzane, France, 2018b.
- N. Tran, F. Rémy, H. Feng, and P. Féménias. Snow facies over ice sheets derived from Envisat active and passive observations. *IEEE Trans. Geosc. Remote Sens.*, 46 (11):3694–3708, 2008.
- N. Tran, F. Girard-Ardhuin, R. Ezraty, H. Feng, and P. Féménias. Defining a Sea Ice Flag for Envisat Altimetry Mission. *IEEE Geosc. Remote Sens. Let.*, 6:77–81, 2009. doi: 10.1109/LGRS.2008.2005275.
- P. Wadhams. Winter Observations of Iceberg Frequencies and Sizes in the South Atlantic Ocean. *J. Geophys. Res.*, 93:3583–3590, 1988.
- D.J. Wingham, C.R. Francis, S. Baker, C. Bouzinac, D. Brockley, R. Cullen, P. de Chateau-Thierry, S.W. Laxon, U. Mallow, C. Mavrocordatos, L. Phalippou, G. Ratier, L. Rey, F. Rostan, P. Viau, and D.W. Wallis. CryoSat: A mission to determine the fluctuations in earth's land and marine ice fields. *Adv. Space Res.*, 37(4):841–871, 2006. ISSN 0273-1177. doi: 10.1016/j.asr.2005.07.027. URL <http://www.sciencedirect.com/science/article/pii/S0273117705009348>. Natural Hazards and Oceanographic Processes from Satellite Data.